TÜRKİYE CUMHURİYETİ
ADANA ALPARSLAN TÜRKEŞ SCIENCE AND TECHNOLOGY UNIVERSITY

GRADUATE SCHOOL
MECHANICAL ENGINEERING DEPARTMENT

OBTAINING BIOGAS FROM MEDITERRANEAN PINE TREE (PINUS PINEA) SEED SHELL AND PLASTIC CATALYST SEED SHELL MIXTURE WITH PYROLYSIS PROCESS

NURİ YÖNET

Ph.D.

ADANA, 2024

TÜRKİYE CUMHURİYETİ
ADANA ALPARSLAN TÜRKEŞ SCIENCE AND TECHNOLOGY UNIVERSITY

GRADUATE SCHOOL
MECHANICAL ENGINEERING DEPARTMENT

OBTAINING BIOGAS FROM MEDITERRANEAN PINE TREE (PINUS PINEA) SEED SHELL AND PLASTIC CATALYST SEED SHELL MIXTURE WITH PYROLYSIS PROCESS

NURİ YÖNET

Ph.D.

THESIS ADVISOR

ASSOC. PROF. DR. ERİNÇ ULUDAMAR

ADANA, 2024

ÖZET

OBTAINING BIOGAS FROM MEDITERRANEAN PINE TREE (PINUS PINEA) SEED SHELL AND PLASTIC CATALYST SEED SHELL MIXTURE WITH PYROLYSIS PROCESS

Nuri YÖNET

Doktora, Makine Mühendisliği Anabilim Dalı

Danışman: Doç. Dr. Erinç ULUDAMAR

Temmuz 2024, 83 sayfa

Bu çalışma, akdeniz çam ağacı tohum kabuğu biyokütlesi ile polietilen katalizörünün pirolizi sonrası ortaya çıkan hidrojen ve metan gazı potansiyelinin araştırılmasını ortaya koymaktadır. Çalışmada öncelikle polietilen malzemelerin viskozitesi, yoğunluğu ve gazdan arınma noktası belirlendi. Tohum kabukları tedarik edilerek piroliz işlemi için ayıklandı. Tohumlar, belirlediğimiz oranlarda katalizör olarak seçilen polietilen malzemeler ile karıştırıldı. Piroliz, 600 °C sıcaklıkta, 50 °C/dakika hızında gerçekleştirildi. Elde edilen gazlar gaz kromatografi cihazı ile analiz edildi. Deneylerin son aşamasında optik mikroskop altında katı kalıntılar gözlemlendi ve mikro yapıları da incelendi. Sonuçlar, akdeniz çamı çekirdeği kabuğu biyokütlesinin ve bunun düşük yoğunluklu polietilen ile karışımının metan ve hidrojen gazları üretebileceğini gösterdi. En düşük viskozite değerlerinden (0,45 gr/10 dk.) ve en yüksek yoğunluk değerlerinden (0,950 gr/cm3) birine sahip olan M8 katalizörü en yüksek metan ve hidrojen gazı verimini sağlamıştır. Piroliz deneylerinde Akdeniz çam ağacı tohum kabuğu biyokütlesinden %38,44 CH_4, %19,50 CO_2 ve %42,06 H_2 gazları elde edilmiştir. Ayrıca biyokütlenin CO_2 emisyon değerleri hesaplanmış ve DEFRA değerleri ile karşılaştırılmıştır. Çalışma, piroliz işlemi yoluyla hidrojen ve metan elde edilebildiğinden, akdeniz çam ağacı tohum kabuğunun yeni bir biyokütle kaynağı olarak sınıflandırılabileceğini ve içten yanmalı motorlar için fosil bazlı yakıtlara alternatif yakıt potansiyeline sahip olduğunu gösterdi.

Anahtar Kelimeler: Polietilen Katalizörü, Akdeniz Çam Ağacı Tohumu, Piroliz, Hidrojen, Metan

ABSTRACT

OBTAINING BIOGAS FROM MEDITERRANEAN PINE TREE (PINUS PINEA) SEED SHELL AND PLASTIC CATALYST SEED SHELL MIXTURE WITH PYROLYSIS PROCESS

Nuri YÖNET

Ph.D., Department of Mechanical Engineering

Supervisor: Assoc. Prof. Dr. Erinç ULUDAMAR

July 2024, 83 pages

This study reveals the investigation of the hydrogen and methane gas potential resulting from the pyrolysis of Mediterranean pine tree seed coat biomass and polyethylene catalyst. In the study, firstly, the viscosity, density and degassing point of polyethylene materials were determined. Seed shells were supplied and sorted for the pyrolysis process. The seeds were mixed with polyethylene materials selected as catalysts in the proportions we determined. Pyrolysis was carried out at a temperature of 600 °C at a rate of 50 °C/min. The obtained gases were analyzed with a gas chromatography device. In the final stage of the experiments, solid residues were observed under an optical microscope and their microstructures were also examined. The results showed that mediterranean pine core bark biomass and its blend with low-density polyethylene could produce methane and hydrogen gases. The M8 catalyst, which has one of the lowest viscosity values (0.45 g/10 min.) and the highest density values (0.950 g/cm3), provided the highest methane and hydrogen gas yield. In pyrolysis experiments, 38.44% CH_4, 19.50% CO_2 and 42.06% H_2 gases were obtained from the Mediterranean pine tree seed coat biomass. Additionally, CO_2 emission values of biomass were calculated and compared with DEFRA values. The study showed that since hydrogen and methane can be obtained through the pyrolysis process, mediterranean pine tree seed husk can be classified as a new biomass source and has potential as an alternative fuel to fossil-based fuels for internal combustion engines.

Keywords: Polyethylene Catalyst, Mediterranean Pine Tree Seed, Pyrolysis, Hydrogen, Methane

Dedication

I dedicate this thesis to my mother Aynur Yönet and my father Ayhan Yönet, who passed away in the February 6, 2023 Earthquake.

Additionally, I dedicate it to my daughter İnci and my wife.

ACKNOWLEDGEMENTS

I would like to thank my advisor, Assoc. Prof. Dr. Erinç ULUDAMAR, for his unwavering support during my doctoral education and thesis work.

I would like to thank Assoc. Prof. Dr. Gökhan TÜCCAR for his unwavering support throughout my education.

I would like to thank Assoc. Prof. Dr. İlyas KACAR from Niğde Ömer Halisdemir University for his support during my experimental studies.

I would like to thank Assoc. Prof. Dr. Hüseyin Turan ARAT from Sinop University, who contributed to my academic life.

I would like to thank all my Jury Member Professors who supported me in my thesis defense.

I would like to thank all the power of the university and the professors who supported me throughout my education.

TABLE OF CONTENTS

LIST OF FIGURES

LIST OF TABLES

LIST OF ABBREVIATIONS

PE	:Polietilen
PP	:Polypropylene
HDPE	:High Density Polyethylene
LDPE	:Low Density Polyethylene
LPG	:Liquefied Petroleum Gas
PET	:Polyethylene Terephthalate
PS	:Polystyrene
MFI	:Melt Flow Index
OMWS	:Olive Mill Wastewater Sludge
DB-SOFC	:Direct Biofuel Solid Oxide Fuel Cell
HHV	:Higher Heating Value
CMAP	:Continuous Microwave-Assisted Pyrolysis
GC	:Gas Chromatography
GC-MS	:Gas Chromatography And Mass Spectrometry
TGA	:Thermogravimetric
XPS	:X-Ray Photoelectron Spectroscopy
NOX	:Nitric Oxide
K	:Potassium
Ca	:Calcium
CeO_2	:Cerium Oxide nano powder
N_2	:Molecular Nitrogen
CH_4	:Methane
H_2	:Hydrogen
CO_2	:Carbon dioxide
KOH	:Potassium hydroxide
Fe	:Iron
CaO	:Calcium oxide
Ni	:Nickel
ZnO	:Zinc oxide
Na_2CO_3	:Sodium carbonate
$ZnCl_2$	:Zinc chloride

LIST OF SYMBOLS

g	**:** gramme
cm^3	**:** cubic centimeter
min	**:** minute
t	**:** time
d	**:** density
mol	**:** molecular
C	**:** celsius

1. INTRODUCTION

Industrialization and population growth have increased energy consumption significantly every year [1]. With developing technological equipment, people have also become dependent on energy. Fuel energy, especially electrical energy, has gained an important place in people's lives. Energy resources, which have become indispensable for the continuation of daily life activities, have given rise to the need for alternative energy sources in terms of their usability, accessibility and ease of acquisition. Since this demand is largely met by fossil fuels, the ecological balance of nature is noticeably disrupted by everyone [2]. For environmental, economic and political reasons, researchers have been searching for environmentally friendly and sustainable energy sources for countries for decades. When fossil fuels are mentioned, what comes to mind is; Gasoline, diesel and LPG (liquefied petroleum gas) fuels stand out as classical fuels. It has been determined that there may be problems in obtaining fossil fuels in the coming years and that they are not sustainable [3]. Among sustainable energy sources; Wind gas energy, solar energy, wave energy (tidal), hydroelectric energy, geothermal energy and biomass energy sources are a few of them [4].

Biomass is a natural resource that, as a group of wastes, can be easily converted into an energy source and appears as a sustainable energy source. It is an effective renewable energy source in increasing energy efficiency and reducing emissions[5]. Likewise, the combustion feature of biomass energy increases economic sustainability and protects the environment. These types of fuels store the energy captured by the sun during photosynthesis. Biomass is a promising alternative fuel to fossil-based fuels [6]. The diversity of renewable energy sources according to years is given in Figure 1.1.

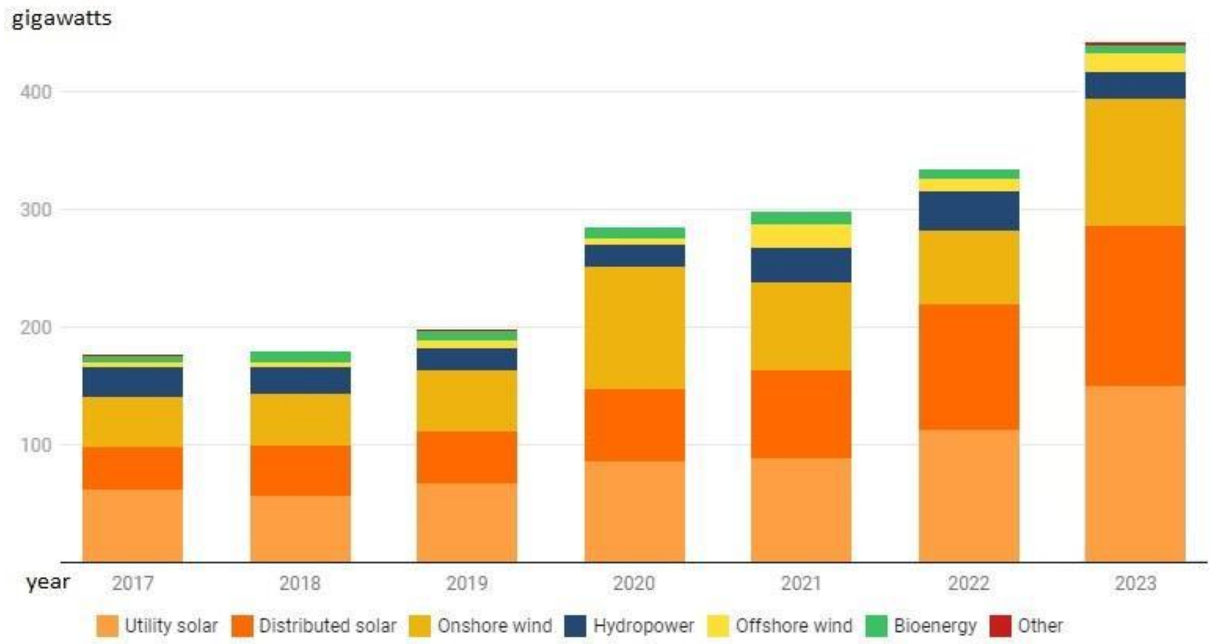

Figure 1.1. Renewable Energy Sources [7]

At the distribution of renewable energy sources based on electrical energy production, it is seen that the use of solar energy is increasing. However, the importance of bioenergy resources can be seen in Figure 1.1.

The efficiency and availability of renewable energy resources over time in the coming years are given in Figure 1.2. At the graph, it can be seen that solar energy will continue to increase its popularity in the coming years. It is known that the need for energy resources will continue to increase every year. In response to the need for existing energy sources, it is predicted that new renewable energy sources may emerge by 2030.

At the graphs, it can be seen that there are many renewable and sustainable energy sources that can be alternatives to fossil fuels. New energy sources will continue to emerge instead of energy sources that can be used as fuel, especially in vehicles used for transportation purposes. Biomass, which is also the subject of study among renewable and sustainable energy sources, has great importance.

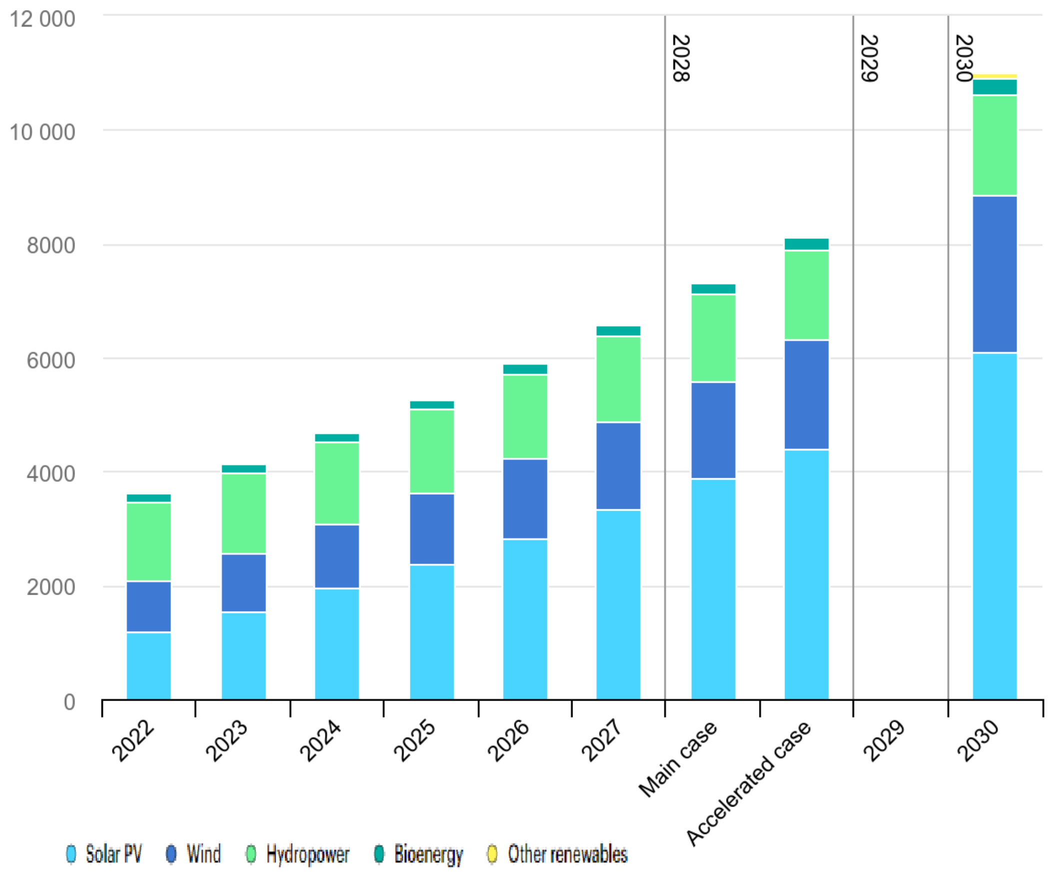

Figure 1.2. Future Scenario on Renewable Energy Sources [8]

There are different methods to obtain sustainable energy sources. Wind turbines are used for wind energy, solar energy systems for solar energy systems, hydroelectric systems for water-based energy production, and biochemical technologies for bioenergy production. Biochemical technologies and thermochemical technologies are used for bioenergy conversions [9]. There are four main thermochemical processes to convert biomass into biofuels; these; roasting, combustion, gasification and pyrolysis. The drying process is used as a heating method to remove water from the product. The combustion process completely burns the product in an oxygenated environment and the properties of the remaining solid product are examined. In the gasification process, the gases obtained from the product heated rapidly at a certain temperature are examined. In the pyrolysis process, the product is heated at different speeds up to a certain temperature in an oxygen-free inert environment and all solid, liquid and gas residues are examined after the process. Although the pyrolysis method has similar characteristics to the gasification method, it is a method in which wide-ranging results about the product can be investigated. Pyrolysis method is also a common method used to convert biomass into bioenergy.

Pyrolysis is one of the thermochemical processes that undergo thermal degradation of animal wastes (cattle, chicken, pigs, sheep, etc.), industrial wastes (slaughterhouse waste, blood, fish waste, etc.), agricultural wastes (corn and corn cobs, wheat straw) [10]. The mechanism of the basic pyrolysis system that can be created is shown in Figure 1.3.

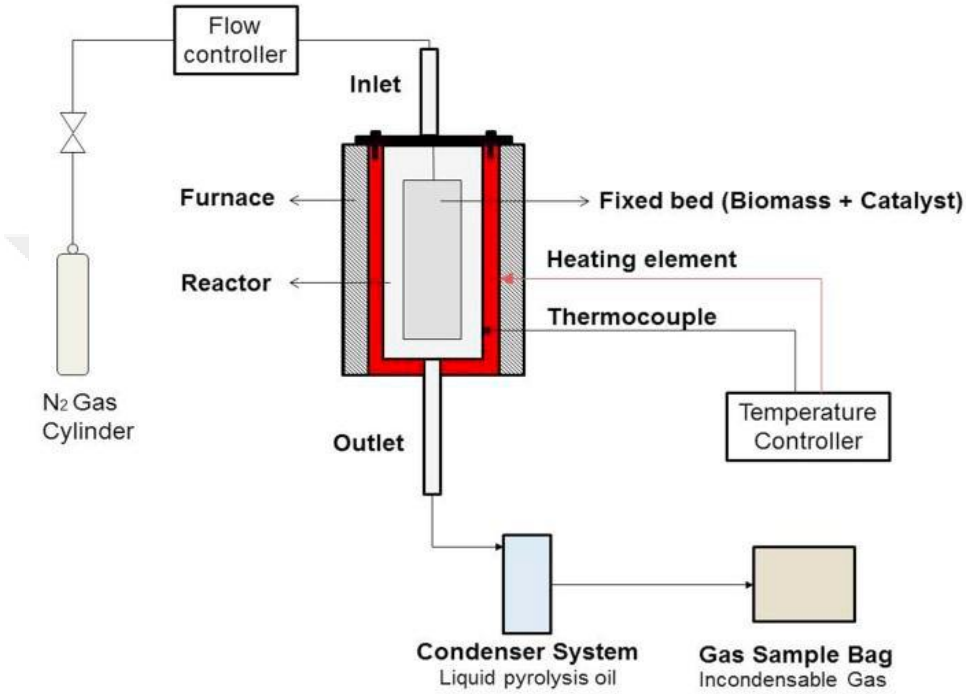

Figure 1.3. Basic Pyrolysis System [11]

When we look at the pyrolysis system, it can be seen that N_2 gas is used as an inert gas to create an oxygen-free environment. In the system mechanism, there is a closed environment that does not come into contact with the external environment, and gas, liquid and solid product intake points that will be formed after pyrolysis. For pyrolysis, an electronic control system is created to monitor the amount of heat and heat duration in a controlled manner.

It has been proven in most studies that the results of pyrolysis experiments with pine groups are effective. It has been observed that white pine wood has high calorific values after pyrolysis output [12]. It is seen that the woody properties of pine trees can be pyrolyzed and gas can be obtained, with the effect of their cellulosic structure, without being exposed to combustion, and with the contributions of the living organisms present in their content.

Another group of materials for which the pyrolysis system can be applied is the group of plastics with thermoplastic properties. Polyethylene (PE) thermoplastic materials are also known as a conversion of fossil fuels. PE groups are petroleum based products. Final plastic materials can be produced from pure thermoplastics or from waste plastic groups. Especially in plastic injection and extrusion production methods, gas release occurs from plastic materials during exposure to heat.

CH_4 and H_2 can be produced from the pyrolysis of solid wastes. When the material is exposed to high temperatures, it breaks down chemically and physically in the absence of oxygen. Decomposition occurs due to the limited thermal stability of the materials' chemical bonds, allowing them to be broken down by heat. It enables the purchase of products with a different, often superior, character than the original relic. Pyrolysis products always produce solid (coal, biochar), liquid and non-condensable gases (hydrogen, natural gas, carbon monoxide, carbon dioxide and nitrogen). In the category of agricultural products where pyrolysis can be applied, it is present in woody products. Gas extraction studies using the pyrolysis method have been carried out on a variety of materials, including animal waste, industrial byproducts, agricultural residues, and surface crusts of woody materials. While some research focuses on the red pine family as the source of gases obtained from the pine tree, others attempt to obtain gas by blending polypropylene plastic materials with metal alloys.

No study has been reported on the pyrolysis of pine seed bark from the Mediterranean region, which is the subject of our study, with a catalyst. For this reason, in this thesis study, pine seed shell materials from the Mediterranean region are examined by applying pyrolysis.

The aim of this study is to produce environmentally friendly and sustainable flammable methane and hydrogen gas that serves as an alternative to fossil fuels, using a biomass product that has not been previously documented in the literature. Uncertainties about the sustainability of fossil fuels and the amount of stocks in the coming years have accelerated the search for new energy sources. Easy access to new energy sources and methods of obtaining them may also vary. Among the controllable and producible energy sources, wind energy, solar energy, biomass energy, hydrogen energy and hydropower plant energy are increasing in popularity. In this study, the energy source potential of biomass was once again demonstrated by choosing the method of obtaining energy from biomass, ensuring the prevalence and sustainability of biomass. It has been demonstrated that woody biomass can be used as an energy source in regions where forests are dense. The high rainfall rate and the presence of dense forest areas in the Mediterranean region show that woody biomass is an easily accessible product for academic research. It has been proven that biomass energy potential can be investigated with experimental setups that can be set up in a laboratory environment. The pyrolysis method was preferred as a method that can yield multiple results with multiple variances. By establishing a fast, easy and traceable experimental setup, the pyrolysis method was established in a laboratory environment, and the feasibility of energy conversion of Mediterranean pine seed shells in industrial pyrolysis systems was proven.

The use of recycled polyethylene and pine seed shells as materials makes our study different as these specific combinations are proposed for the first time in this thesis study. This uniqueness adds innovative features to our study, facilitating easy comparison with other research results.

2. THEORETICAL FOUNDATIONS AND LITERATURE REVİEW

In the literature studies carried out within the scope of the thesis study, studies on the applications of the pyrolysis system were encountered. There are also woody materials in which the pyrolysis method is used. Outputs of pyrolysis products, especially after mixing with catalyst materials, are also available.

Al-Fatesh et al. (2023) states that the pyrolysis process is affected by the composition of the material being processed, particle size and process temperature [13]. Additionally, catalyst loading and the duration of the material remaining in the chamber also affect pyrolysis [14].

Various catalysts have been investigated for the pyrolysis and gasification of plastic and biomass. Of these, the formation of hydrogen-rich gas from the pyrolysis-gasification of a hazelnut shell and polypropylene mixture with the Fe/CaO/Ni/mayenite/CeO_2 (1:1:1:1:2) catalyst was studied by Oni et al. (2023). They concluded that at 1000 °C, 30 wt% catalyst increased hydrogen production as the pore volume, surface area, and porosity increased with the addition of catalyst [15].

Tian et al. (2023) investigated the air gasification of pine sawdust on Ni/olivine catalyst. They achieved 72.4% gas yield with Ni/olivine at an equivalence ratio of 0.21. They also found that the H_2 concentration increased at high temperature [16].

Acevedo-Paez et al. (2023) showed that in non-catalyzed gasification, the highest H2 content reaches approximately 34 mol%, while in catalysts this ratio varies between 40 and 73 mol%. Catalysts grafted with Ni, Ca, and K exhibited the highest H_2 content of 72.9 mol% [17].

Yue et al. (2023), biomass energy was obtained from the pyrolysis of corn stover on Ni/Ca catalyst. They reached the highest pyrolysis gas yield of 661.63 mL/g biomass, accompanied by the highest H_2 concentration of 68.62% by volume, biomass yield of 450.15 mL/g and conversion rate of 65.97% by weight [18].

Another contribution of biomass products is that they provide an alternative to other energy sources that cause global warming and climate change [19]. For this reason, in recent years, many researchers working on biomass products have focused on reducing the carbon footprint.

Fu et al. (2024) mixed corn straw-eucalyptus sawdust-apple sawdust and conducted a slow pyrolysis experiment at 700 °C to check the NOx precursor, char-N, tar-N and their properties. They examined these using GC-MS, TGA, XPS and spectrophotometry. They concluded that the addition of eucalyptus wood chips increased char-N yield. The synergistic intensity was strongest at -0.5926 with the addition of 25 wt% Eucalyptus wood chips, while the apple wood synergistic strength was strongest at -0.5798 with the addition of 50 wt% [20].

Different waste Accoutrements contribute to the gasification of biomass. These complements may also vary depending on the type of synthetic, cellulosic and woody material. Hydrogen metamorphoses can also be covered by observing the conformation of CH_4 and H_2 during the pyrolysis of biomass. Li etal. (2024) conducted a study illustrating this change and set up that gas effectiveness increased by 10.30-38.90, H_2 effectiveness increased by 17.31-81.40, and biomass containing advanced attention of cellulose and hemicellulose increased in gas product. revealed that it performs better [21].

In the literature, gas effectiveness and gas conformations are observed by creating different atmospheric surroundings. Two- stage fast pyrolysis of waste cuisine oil painting and sludge stover biomass under CO_2 atmosphere to produce hydrocarbon-richbio-oil was delved by Wu et al.(2024). CO_2 and N_2 feasts were used at different stages to produce an oxygen-free terrain. This study, combined with CO_2 supported pyrolysis and waterfall pyrolysis, presented a new idea of thermal conversion of waste cuisine oil painting and sludge stover to produce hydrocarbons [22].

Chen etal.(2024) estimated product distribution and synergistic goods duringco-pyrolysis of agroforestry remainders and polyethylene terephthalate and polypropylene wastes. Thermogravimetric analyzer results showed that the corruption of biomass has stages of water evaporation, evaporation and solid corruption; Fourier transfigure infrared spectroscopy showed that biomass and plastics have analogous functional groups; Pyrolyzer- Gas chromatography/ Mass spectrometry showed that biomass- PETco-pyrolysis increased carbohydrate and ester conformation but inhibited phenol conformation [23].

In addition to carrying CH_4 by pyrolysis system, it can also play an active part in carrying H_2. Hydrogen product from biomass of used lithium ion battery cathode accoutrements was tried by Yu et al. (2024). They set up that the hydrogen yield of the cathode material by coconut shell carbon reduction at 800 °C was 24.9 mmol/g. With better dissipation of cobalt, a advanced hydrogen yield of 28.3 mmol/ g was attained. The study showed that spent lithium- ion battery cathode accoutrements give a suitable route to apply them in the product of hydrogen from biomass [24].

Parparit etal., thermal geste of different biomass types similar as eucalyptus globulus sawdust, thermomechanical pulp of Norway improve(Picea abies); Brassica rapa and its derivations, pine cones, grape seeds were estimated by thermogravimetry and logical pyrolysis. Liquid products attained from pyrolysis were anatomized with different modules of the gas chromatography device. essential analysis and spicy values of pyrolysis remainders were delved . The performing pyrolysis products; It has been determined that it consists of carboxylic acids, ketones, furans, phenols, guaiacols, catechols and their derivations. The content of composites in canvases largely depends on the biomass source It has been observed that there are differences in pyrolysis geste between biomass samples [25].

In the study conducted by Elleuch (2018) and his associates, named disquisition of the complex electrochemical and chemo-mechanical geste of solid oxide energy cell fueled with pyrolysisbio-oil; Direct use ofbio-oil of olive shop wastewater sludge (OMWS) set via fast pyrolysis in Direct Biofuel Solid Oxide Energy Cell (DB- SOFC) has been delved . Whenbio-oil was hotted , it perished to form feasts, unpredictable substances and solid remainders(biochar). Carbon deposit at 650 ^{o}C was achieved through oxidation with oxide ions and chemical response with CO2 and H2O feasts. Above 700 ^{o}C, a drop in performance was noted due to biochar accumulation at the anode through response creation, increase in O_2 transfer and possible electrochemical oxidations of carbon. They demonstrated that direct fed SOFCs with OMWSbio-oil can be achieved using Ni- SDC anode, but enhancement in energy quality and anode catalytic exertion and stability is needed to significantly ameliorate cell performance [26].

Günay Özbay conducted a study on catalytic pyrolysis of pine wood greasepaint forbio-oil product probing the goods of temperature and catalyst complements. To gain optimum conditions to achieve maximumbio-oil yield,non-catalytic pyrolysis of Turkish pine(Pinus brutia Ten.) wood sawdust was carried out at colorful temperatures in a fixed- bed reactor. Fornon-catalytic pyrolysis, the loftiestbio-oil yield of roughly 46 wt was attained at 550 ˚C. Under optimum conditions, the goods of different catalyst types (KOH, $ZnCl_2$ and ZnO) and catalyst quantities (5, 10, 15 and 20 wt) on pyrolysis product yield andbio-oil parcels were delved . The presence of catalysts significantly changed the product distribution. While adding the quantum of catalyst led to a drop in liquid product yield, it was observed that gas and coal yields increased compared tonon-catalytic pyrolysis. The chemical compositions of biooils were determined by GC- MS analyses. The results showed that biooils could be bettered with a catalyst. For this reason, it has been emphasized that catalyst selection is veritably important for high biooil quality in artificial operations [27].

In the studies of Ayhan Özçifçi and Günay Özbay, Scots pine(Pinus sylvestrisL.) wood sawdust was estimated as a biomass source, and(thermal) pyrolysis with and without catalyst was carried out in a fixed bed reactor. In the trials, the effect of parameters similar as temperature and catalyst type on the yield of pyrolysis products was delved . Pyrolysis of test samples with flyspeck size of0.850-1.60 mm; It was carried out at temperatures of 400, 500 and 600 °C, a heating rate of 5 °C/ min and an enplaning nitrogen gas (N2) inflow rate of 30 ml/ min. Na2CO3 and K_2CO_3 introductory mariners and $FeCl_3$ Lewis acid were used as catalysts. It has been determined that temperature and catalyst type are effective parameters in solid, liquid and gas product yields. It has been determined that liquid products attained from wood sawdust by catalytic pyrolysis system can be used as biofuel or precious chemical substance [28].

A study was conducted in which pine cones and synthetic polymers(PE, PP and PS) were pyrolyzed together. The pyrolysis temperature was chosen as 500 oC. Gas, liquid and solid products from biomass were anatomized by taking pyrolysis products similar as polymer canvases and coal. further liquid products were attained in biomass and polymer admixture pyrolysis than laboratory products. In the study, pyrolysis was also carried out with a admixture of biomass and pure cellulose polymer. It has been observed that in fusions with polymer accoutrements , further gas is formed and lower coal is formed. It was concluded thatco-pyrolysis coals have advanced spicy values compared to pyrolysis of biomass alone [29].

In the study conducted on the pyrolysis of coffee grounds remaining after brewing, it was aimed to experimentally probe the effect of lipid birth and conversion to biodiesel on the energy yield of pyrolysis products. Microwave oven- supported lipid birth system was used and a two- stage transesterification process was considered for conversion to biodiesel. Fast pyrolysis of defatted spent coffee grains was carried out with a 300 g/ h screw reactor at temperatures of 400 °C and 550 °C. The results show a significant effect of pyrolysis temperature on the energy distribution of pyrolysis products. Thenon-condensable gas composition surfaced amended with hydrogen and methane with the increase in temperature. Biodiesel energy donation significantly bettered the energy effectiveness of the pyrolysis system, leading to an increase in energy effectiveness of further than 10 at 550 °C, while furnishing a limited increase of 4 at 400 °C [30].

In the study where the basics of pyrolysis are explained, pyrolysis appears as a thermochemical conversion fashion to produce biofuel from biomass and as a system by which the usability of biofuels to incompletely replace fossil energies can be delved . The product and parcels of liquid, solid and gassy biofuels are affected by numerous factors similar as flyspeck size, temperature, heating rate, gas hearthstone time, atmosphere, pretreatment styles, catalysts and reactors. In particular,bio-oil produced by biomass pyrolysis has undesirable energy parcels and is thus far from a direct relief for fossil energies. So far, colorful approaches of catalytic pyrolysis of biomass and catalytic elevation ofbio-oils have been developed to produce high-gradebio-oil or value- added chemicals. also, further attention has been emphasized on the development of effective andanti-deactivated catalysts, reactors and optimization of the pyrolysis process for large- scale product of liquid energies and fine chemicals [31].

In the study of Jian Zhanga etal. named" Direct conflation of concave carbon nanofibers onbio-char during microwave oven pyrolysis of pine nut shells"; Pyrolysis was applied by creating a compound material. Detailed analysis of volatiles evolved during microwave oven pyrolysis has shown that hydrocarbons inbio-oil, similar as benzene and alkenes, and CO, CO_2, methane and ethane inbio-gas act as carbon sources during the conformation of HCNFs [32].

Nuri Tunç and his associates in their study" Environmental pollution cost analysis of a diesel machine operating with biogas- diesel- tyre pyrolytic oil painting fusions"; Environmental pollution cost analysis was conducted for a diesel machine operating with pyrolytic oil painting-biogas-pure diesel energy fusions. Three different values were anatomized at different rates. In the trials of all products, constant inflow rates of 1, 3 and 5 L/ min were used. It was concluded that energy fusions can be used rather of being diesel energy in diesel machines [33].

Melek YILGIN and her associates, in their study named" Flash Pyrolysis of Wood", delved the flash pyrolysis results of wood species similar as oak, pine and poplar at different temperatures and different grain sizes. Liquid product yield increased with adding pyrolysis temperature and dropped with adding grain size. It has been observed that woody products are effective on pyrolysis product yield. It was observed that the solid product yield was high in oak wood with high lignin content, and the liquid and gas product yield was high in poplar wood with high cellulose content [34].

Antonio Vita and his associates, in their study on the optimal operating condition of biogas and the effect of nickel content as a renewable raw material for conflation gas product bytri-reformation process on Ni CeO_2 catalysts prepared for conflation gas, Ni/ ceria grounded catalysts, product through combustion conflation (nickel content by weight) concentrated on the ternary reformation of simulated biogas at1.8 –31.0 wt. It revealed that some of the nickel was incorporated into CeO_2; The parcels of the CeO_2 support can play an important part in the catalytic exertion and stability of Ni/ CeO_2 catalysts. Among the samples examined, the catalyst loaded with 7.7 wt Ni showed the loftiest catalytic exertion. At 800 °C, the transformations of CH_4 and CO_2 are 98.94 and 89.22. It has also been observed that the molar rate of H_2 and CO can be flexibly acclimated by the quantities of oxygen and brume [35].

Within the compass of the doctoral thesis named" The Effect of Dual Energy(Biogas- Diesel) Use on Performance and Emigrations in a Low Heat Loss Diesel Engine" prepared by İlker Turgut Yılmaz, diesel, methane, 60 methane- 40 carbon dioxide admixture, 80 methane in a standard and thermally insulated machine. -20 carbon dioxide admixture, 80 methane- 10 carbon dioxide- 10 hydrogen admixture energies were used. In the trials conducted, combustion characteristics(injection time, ignition detention, launch of combustion, maximum cylinder pressure, maximum cylinder pressure increase rate, heat generation rate, accretive heat generation, heat generation center), machine performance(power, necklace, outside in-cylinder temperatures, exhaust gas temperatures, volumetric effectiveness, cost analysis, specific energy and specific energy consumption) and exhaust emigrations(HC, CO_2, NOx and soot) were determined. The results attained were compared with the reference values attained by using diesel energy in a standard machine [36].

In the study conducted by Qazi Sohaib and his musketeers; The geste of waste biomass was delved using fast pyrolysis at different times and temperatures. Rice straw, sludge stover, and pyrolysis yields were anatomized using proximal analysis, postanalysis, and gas chromatography. Thebio-oil yield of different biomass was characterized. The results showed that adding the fast pyrolysis temperature over to 500 °C increased thebio-oil and gas yield, while the housekeeper content dropped. A unforeseen increase in gas yield was observed above 450- 500 °C. The increase in temperature increased the attention of H2 and CH4 [37].

In his master's thesis named" Pyrolysis of Some Biomass and Investigation of Pyrolysis Products", Ahmet OLGUN stated that the loftiest temperature attained at 450 °C for hornbeam, 350 °C for oak and 450 °C for poplar with 1- hour pyrolysis in the temperature range of 300-450 °C. Gas product yields are65.05,47.60,35.59 independently. At 450 °C pyrolysis temperature, the loftiest gas product yield for hornbeam was attained as65.05 in 1 hour of operation. At 450 °C pyrolysis temperature, the loftiest gas product yield for oak was45.84 in1.5 hours of operation, and the loftiest gas product yield for poplar was54.29 in half an hour of operation [38].

Hayati OLGUN and his associates, in their study named" Use of Solid Waste in Energy Conversion and Gasifiers", conducted gasification trials of hazelnut shells and gave theresults.However, 2, If 1 kilogram of hazelnut shells with 13 humidity is burned.45 m3 of ignitable gas is produced. In other words, 1.2 kg of hazelnut shells can produce enough gas to produce 1 kW of electrical energy and 5 kW of heat energy per hour [39].
As a result of the pyrolysis system applied at different temperatures on the dinghy and branches of the beech tree, Mathieu Morin and his associates revealed that an increase in the pyrolysis temperature leads to an increase in the carbon content and a drop in the oxygen and hydrogen content. also, watercolor performing from fast pyrolysis of beech dinghy bullet is more reactive than watercolor attained from fast pyrolysis of beech stick [40].
In the study conducted by Erinç Uludamar and his associates on the effect of natural gas and biodiesel energy fusions on exhaust emigrations, natural gas was used as the secondary energy in the machine trials, and low sulfur diesel energy and its admixture with sludge biodiesel (20 and 40 by volume) were used as the primary energy. While biodiesel composites handed 4.05 and 7.63 lower CO emigrations for CoB20 and CoB40, independently, the preface of natural gas caused a significant increase in emigrations. still, the increase in CO_2 emigrations caused by the addition of biodiesel to low- sulfur diesel energy was well neutralize by the addition of natural gas. In addition, the 4.08 and 18.00 NOx emigration increase performing from the use of CoB20 and CoB40 was compensated up to 33.0 by switching to natural gas [41].
In the studies of Esra Gök and her associates, the pyrolysis of pollinated woody structures of poplar and pine trees and their solid and liquid results were delved . As a result of the study, it was observed that poplar wood grains gave lower yields of solid and liquid results than pine wood grains [42].
Sevzi Şensöz, in her study on the pyrolysis of red pine (Pinus Brutia Ten.) with barkless sawdust, the goods of pyrolysis temperature and heating rate on the product were delved . The temperature was determined to be in the range of 300 to 550 °C and the heating rate to be 7 to 40 °C/ min. The yield of coal, gas and liquid as a result of pyrolysis varied between 23 and 36, 11 and 23 and 21 and 30 by weight, independently. The loftiest liquid yield was attained at 500 °C pyrolysis temperature with a heating rate of 40 °C/ min. A significant increase in pyrolysis conversion due to rapid-fire evaporation was observed in the temperature range of 450 to 500 °C [43].

Tuba Ersen and Dursun Pehlivan, in their study namedCo-Pyrolysis of High Density Polyethylene – Wood fusions, delved theco-pyrolysis of high viscosity polyethylene(HDPE) named from domestic plastic wastes and pine wood greasepaint named as biomass. The goods of different pyrolysis parameters(heating rate, final temperature, sweeping speed, mixing rate) on the yields of the products performing from the fixed bed pyrolysis of bullets prepared from fusions of these accoutrements in certain proportions of the ground samples were revealed. The loftiest liquid product yield was attained at a heating rate of 5 ^{o}C/ min, in a nitrogen-free terrain(an terrain where nitrogen enplaning gas wasn't used and expressed as 0 mL/ min) and at a pyrolysis temperature of 700 ^{o}C [44].

Neslihan Doğan- Sağlamtimur and her associates subordinated end- of- life tire and polyethylene terephthalate (PET) bottle wastes to a thermodynamic process with their recently designed pyrolysis reactor. In the study, 4- stage separation(200, 250, 300 and 350 ^{o}C), 5-stagepre-concentration with a cooler machine(- 20,-10.0, 10 and 20 ^{o}C) and final attention were applied. At the corruption temperature of 300 ^{o}C, the end- of- life rubber reached a pasty thickness, but couldn't gasify and thus couldn't condense. At the corruption temperature of 350 ^{o}C, gasification started and consequently, in four condensation way(- 10, 0, 10 and 20 ^{o}C), the solid product (carbon dark) increased in the range of 232- 256 g, and the liquid product (pyrolytic oil painting) increased in the range of 50, 54 g. It was attained as 32 and 28 mL [45].

İlknur Demiral and associates applied the pyrolysis system to produce biofuel from the soft shell of pistachio(Pistacia veraL.). The goods of temperature, heating rate and reach gas (N2) inflow rates on the yields and compositions of the products were delved . Pyrolysis studies were carried out using reactor temperatures between 350 ^{o}C and 500 ^{o}C with heating rates of 15 ^{o}C and 50 ^{o}C = min. Chemical characterization has shown that biooil attained from the soft shell of pistachios can be used as a renewable energy and chemical feedstock [46].

Gülbahar Okay and her associates carried out pyrolysis trials on the atrophied woody structures of pine and poplar trees. As a result of the woody structures tested under pyrolysis temperatures of 450 ^{o}C, 550 ^{o}C and 650 ^{o}C, the temperature at which the maximum liquid product yield attained for both products was determined as 550 ^{o}C. While the solid product yield dropped with a temperature of 650 oC, it was observed that the liquid product yield dropped at advanced temperatures [47].

İbrahim Üçgül and Ufuk Elibüyük estimated the pyrolysis labors of cloth wastes using the pyrolysis system. Acrylic, cotton and hair fiber wastes were subordinated to pyrolysis and the solid products performing from this process were estimated. It was observed that during the pyrolysis process, no solid product was formed in cotton fiber, but solid wastes of tempera and hair were formed [48].

In their study, Tabakaev etal. examined the thermal goods observed in low- temperature pyrolysis and estimated the possibility of autothermal biomass processing. Straw from two beds of the Tomsk region(Russia), sawdust from colorful tree species, pine sawdust and peat were considered biomass. A physical trial, discriminational thermal analysis, gas chromatography and heat balance equations were used in the study. It was established that low- temperature pyrolysis of biomass is accompanied by a positive value of the thermal effect in the temperature range of 220 – 580 ^{o}C and varies from 393 to 1475 kJ kg- 1 depending on the type of raw accoutrements reused.. The value of this effect makes it possible to organize the pyrolysis of biomass in an autothermal governance with primary drying the maximum humidity content for straw is 19.9, for sawdust 10.4, for sawdust 9.7 and for Sukhovskoy peat 9.5 [49].

In the thesis study conducted by Mustafa Salih Budak, the liquid product performing from the catalytic depolymerization of powdered calcined wood chips in a admixture of catalyst, lime and waste oil painting using slow and fast pyrolysis ways was examined. The heating rate and high temperature in the catalytic declination of wood chips caused an increase in liquid and gas product yields and a drop in solid product yields. It has also been observed that the yield of liquid and gassy products increases in the presence of waste oil painting, lime and catalyst [50].

Asa Ingemarsson and his associates performed slow pyrolysis trials with sharp and pine samples. Small samples (10 to 150 mg) of eight pine and improve species were pyrolyzed at 550 °C. Samples were taken from Scots pine, Austrian pine, Lodgepole pine, Ponderosa pine, Norway improve, White improve, Black improve and Sitka improve. composites produced from pyrolysis were anatomized by several gas chromatographic (GC) styles. Product distributions of organic composites attained from different conifers show common characteristics. Aldehydes, acids, ketones and methoxylated phenols form large quantities of oxygenated organic composites. Pine species produced less methoxylated phenol than improve species [51].

In light of the knowledge gap in the scale- up of microwave oven- supported pyrolysis technology, this study developed a nonstop microwave oven- supported pyrolysis (CMAP) system and examined its feasibility for conflation gas product. Wood bullets were subordinated to pyrolysis at colorful temperatures in the system and product distribution and energy effectiveness were delved . At a processing temperature of 800 °C, the CMAP system produces a high quality patron gas(low heating value of 18.0 MJ/ Nm3 and syngas content of 67 vol) with a yield of 72.2 wt or 0.80 Nm3/ kgda.a.f.) achieved. Wood outperforms numerous conventional pyrolysis processes, probably due to two factors 1) microwave oven irradiation-enhanced responses between the primary navigator and biochar and 2) the absence of a carrier gas in the process. The energy effectiveness of the process was also estimated. Potentially, electricity consumption could be reduced from 7.2 MJ to 3.45 MJ per kg of wood, allowing for net electricity product from the process [52].

3. METHODOLOGY

The thesis is based on the production of biogas by pyrolysis method by mixing Mediterranean pine seed coats and seed coats with PE catalyst materials. Within the scope of this study, detailed information is given about the supply of pine seeds and making them suitable for analysis, the supply and classification of PE material, analysis devices, methods, standards and applications.

3.1. Pine Seeds

Mediterranean pine seeds were sourced from local suppliers as shown in Figure 3.1. Care was taken to ensure that the seeds supplied were fresh and seasonal. It has been noted that the fresh seeds inside should not be dry. The supplied seeds were broken and took the shape shown in Figure 3.2. The purpose of cracking the seeds is to expel the moisture of the inner seed and preserve the fatty tissue.

Figure 3.1. Shelled Mediterranean pine seeds

Figure 3.2. Broken shelled Mediterranean pine seeds

Mediterranean Pines are from the Pinus Pinea family and are a type of coniferous tree that can grow up to 20-25 meters in length. It reaches maturity in approximately three years and contains its seeds in cones [54]. The average moisture content, protein, oil, ash and dietary fiber values of pine seeds in Turkey were calculated as 3.9, 34.8, 42.9, 4.1 and 13.1, respectively [54].

3.2. Catalyst Materials

PE plastic materials were supplied with samples taken from local manufacturers. A total of 11 PE materials were supplied. The PE materials supplied in the packages, the material flow index (MFI) values and the materials supplied to determine their densities are shown in Figure 3.3.

Figure 3.3. PE materials supplied

10 of the PE materials supplied are in the PE group obtained from recycled materials. One pure PE material was also supplied for analysis and MFI, density value comparison (Figure 3.4.).

Figure 3.4. Pure PE Material

Pictures of recycled PE materials are given below in Table 3.1.

Table 3.1. Recycled PE Materials

		
		
		
		

PE (polyethylene) materials are classified as recycled high-density polyethylene (HDPE) and recycled low-density polyethylene (LDPE) according to their properties. Recycled HDPE materials used in this study include plastic waste such as water cans, bottle caps, food bottles, and kitchen utensils. LDPE materials include plastic waste from transport containers and greenhouse covers.

3.3. Devices and Equipment

3.3.1 MFI Device

It is an MFI analysis based on fluidity, which is the basic feature of the PE materials we choose as catalyst materials. This analysis is performed with the MFI device according to ISO 1133 standards. The device used for MFI values is a domestically produced device of the OMRAN brand. The device image is given in Figure 3.5.

Figure 3.5. MFI Device

The device is a device with a sample capacity of 5 grams, which can heat it to a temperature above the melting or softening point and force it to flow with the help of a piston and weight (usually 2.16 kg or 5 kg) in a sleeve. The weight of the melt released in 10 minutes is the melt flow index value.

3.3.2 Density Meaurement Device

Another important value of PE materials is their density value. Density values of PE material are a determining factor in the usage area of the material and the production process. It has an important place in the production methods and flexibility of products such as canisters, barrels, transport cases, household goods and toys. Density values are determined in density devices by comparing the density with the density of a certain liquid or another material. Density analyzes are performed according to ISO 1183 standard. In the thesis study, RADWAG brand AS 220.R2 model density device was used. The product used by the device for density comparison is ethanol. It determines density according to the density of ethanol. The device image is given in Figure 3.6.

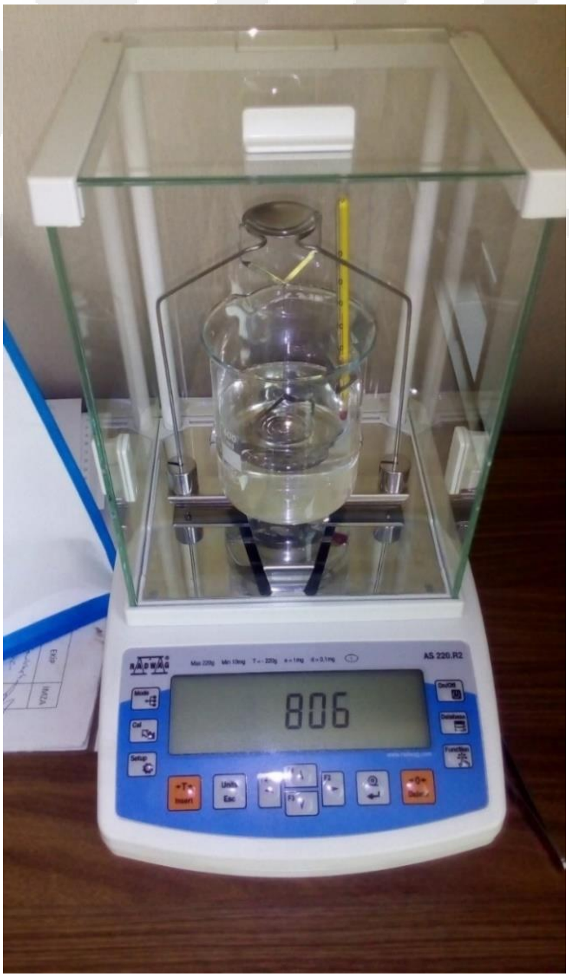

Figure 3.6. Density Measuring Device

3.3.3 Gas Measurement Detector

The gas measuring device warns whether there is gas escaping from the product at the start of the experiment in the pyrolysis device. According to the signal of the device, it was used to understand that the gas flow has started and the gas storage process should be started. If the device detects 200 ppm or more CH_4 (methane) in the environment, the LED alarm lights up yellow; if it detects 10,000 ppm or more CH_4, the LED alarm lights up red. It has the feature of detecting CH_4 in the range of 0-10,000 ppm. It helps detect methane, propane and hydrogen gases. The device visual is given in Figure 3.7.

Figure 3.7. Gas Measurement Detector

3.3.4 Thermometers

During the experiment, more than one digital thermometer was kept to control the temperature of the pyrolysis system and to confirm the digital thermometer of the pyrolysis system. Thermometers with laser measurement, contact surfaces and those that can measure in capillary channels are preferred. Experiments were carried out with devices that could obtain measurement results between -160 °C and 1372°C. Thermometers are given in Table 3.2.

Table 3.2. Thermometer Images

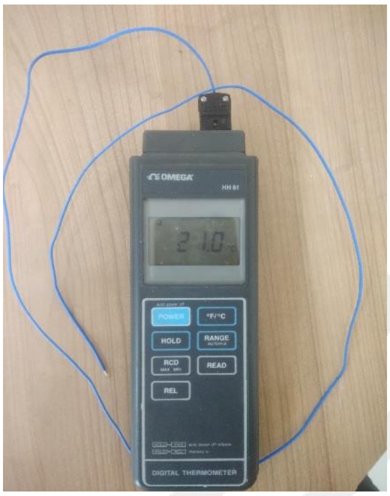		

3.3.5 Glove

After the pyrolysis experiment, heat-resistant gloves are needed when removing the completed sample from the oven. Considering that the pyrolysis temperature reaches +600 °C, it is known that a glove is required to hold the transport container for a short time. The glove used during the experiment is made of dense and dense cotton material and can withstand temperatures of +250 °C. The glove image is given in Figure 3.8.

Figure 3.8. Heat Resistant Gloves

3.3.6. Furnace

An oven was preferred in order to reach the pyrolysis temperature with homogeneous distribution and to maintain optimum parameters along with pyrolysis speed and waiting times. The furnace is a muffle furnace with a temperature of 1200 oC, electric resistance heating, adjustable thermostat adjustment, and a 5-liter chamber. For the pyrolysis experiment, the furnace was redesigned and the nitrogen entry point was opened, and the exit point for the gas obtained from pine seeds was determined. In the thesis study, PROTHERM brand oven was used. The visual of the oven is given in Figure 3.9.

Figure 3.9. Pyrolysis Furnace

In addition to the furnace, the spare retort mechanism shown in Figure 3.10., which includes gas storage, pressure monitoring and gas intake points, has also been added.

Figure 3.10. Pyrolysis Retort Device

3.3.7. Gas Chromatography (GC) Measurement Device

Gas chromatography technique is applied to separate the chemical components of a sample and reveal the existing components. This technique is performed with a gas chromatography device. Chemical components are usually organic molecules or gases. The GC device is connected to the computer via an electronic control unit. The component outputs of the device are graphed by computer. In the analysis results, the components in the sample are named. In the thesis study, Agilent Technologies brand 7820A model GC device was used. The image of the device is given in Figure 3.11.

Figure 3.11. GC Measurement Device

3.3.8. Microscope

Solid products may form after pyrolysis analysis. The solid products formed are carbonized or nearly carbonized before combustion, depending on the pyrolysis time and pyrolysis temperature. The microstructures of the surface movements of these products after pyrolysis can be examined with laboratory microscopes. In our thesis study, pine seed surfaces were examined before and after pyrolysis. In the study, Olympus brand BX51M model microscope was used. The microscope image is given in Figure 3.12. The magnification of the optical microscope was set to X5 or X10 to observe the carbonization status of the outer shell surface and inner oilseed of the biomass.

Figure 3.12. Microstructure Microscope Device

3.3.9. Gas Sample Bag

Gas sample bags were used to store and transport the gases released from the system after the pyrolysis test to the laboratory. Especially those made of aluminum, they are resistant to puncture and the external environment. Their heat-resistant structure makes it easier to preserve gas for a long time. The gas storage bag used in the thesis study is shown in Figure 3.13.

Figure 3.13. Gas Storage Bag

3.3.10. Gas Sample Tube

In order to analyze the gas samples resulting from pyrolysis in the GC device after being stored in gas storage bags, 5ml capacity gas sample tubes, which can also be used in the GC device, were used. Gases were taken into sample tubes with the help of a syringe and could be analyzed in the GC device. Empty, leak-proof blood tubes that do not contain any chemicals were preferred as gas sample tubes. Gas sample tubes are shown in Figure 3.14.

Figure 3.14. Gas Sample Tubes

3.4. Pyrolysis Experiment

For the pyrolysis experiment, the experimental setup given in Figure 3.15. was set up. For equal temperature distribution, there are resistance resistors covering all sides of the system. Liquids that may have formed as a result of condensation during pyrolysis were collected with the liquid collection container. For the pyrolysis experiment, the oxygen-free environment was removed with nitrogen gas. After each experiment, the experimental setup was ventilated to eliminate the effect of the previous pyrolysis gas.

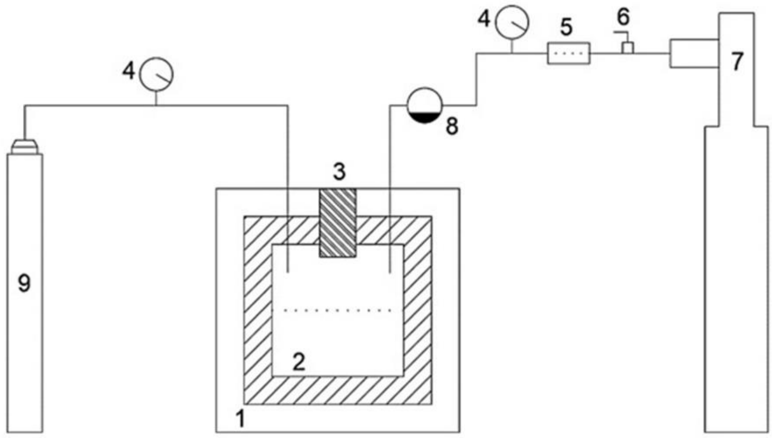

1	Heat Source
2	Pressure Container
3	Safety valve
4	Vacuum Manometer
5	Moisture Trap Filter
6	Gas Control Valve
7	Gas Storage Tank
8	Liquid Collection Cup
9	Nitrogen Tube

Figure 3.15. Pyrolysis Experiment Setup

In this study, slow pyrolysis (temperature range of 450-650 ^{o}C) was used to increase the amount of gas extracted [55]. The experiments were carried out in a laboratory environment using a resistance furnace that can reach up to 1000 °C. The exit of the furnace was from the top and bottom. For the experiments, the samples were placed in the oven without preheating. During the experiments, the oven was heated to 600 ^{o}C with a heating rate of 50 oC/min. After reaching the experimental temperature, the sample was kept for 10 minutes. The exit gas was measured by a gas measurement detector and the samples were taken into a 500 ml capacity degassing vessel for further processing. The chemical content of the obtained gases was analyzed with GC (Gas Chromatography), Agilent 7820A GC device.

In the pyrolysis experiment, mixtures of seed and catalyst materials were mixed and analyzed as shown in Figure 3.16.

Figure 3.16. Catalyst-Seed Mixture

The microstructure of the inner and outer surface of the Mediterranean pine core shell was examined under an optical microscope before and after the pyrolysis experiments.

In the experiments, seeds and polyethylene materials were subjected to pyrolysis separately. Then, for further testing, the seeds and catalyst materials were mixed to create a composite product. In total, 12 different samples were examined and the experiments were repeated three times. The basic equations of the pyrolysis experiment were created by Iwasaki (2003) in his academic study as follows [60].

Basic Pyrolysis Equation:

$C_n H_m O_k \rightarrow (m/2)H_2 + kCO + (n-k)C$ (3.1)

Supplemental Pyrolysis Equations:

$C + 2H_2 \rightarrow CH_4$ (3.2)

$C + H_2O \rightarrow CO + H_2$ (3.3)

$C + \frac{1}{2} O_2 \rightarrow CO$ (3.4)

$C + O_2 \rightarrow CO_2$ (3.5)

$C + CO_2 \rightarrow 2CO$ (3.6)

$CO + H_2O \rightarrow CO_2 + H_2$ (3.7)

4. ANALYSIS AND DISCUSSION

4.1. PE MFI and Density Results

Within the scope of the thesis study, first of all, PE catalyst materials are grouped with the names M1-M11. Values were found with the MFI device. Then, the values of each material were taken with the density measuring device. MFI of PE materials is given in Table 4.1.

Table 4.1. Catalyst PE Calculated MFI Values

Material Code	Material Name	MFI (gr./10 min.)
M1	LDPE- Recycle	1,36
M2	LDPE- Recycle	0,4
M3	LDPE- Recycle	2,65
M4	LDPE- Recycle	1,55
M5	HDPE- Recycle	1,05
M6	HDPE- Recycle	0,84
M7	HDPE- Recycle	0,45
M8	HDPE- Recycle	0,9
M9	LDPE- Recycle	1,77
M10	LDPE- Recycle	1,22
M11	LDPE-RAW	0,30

Density values of PE groups with MFI values are calculated with a density device and shown below in Table 4.2.

Table 4.2. Calculated Density Values of Catalyst PE

Material Code	Material Name	Density (g/cm3)
M1	LDPE- Recycle	0,921
M2	LDPE- Recycle	0,921
M3	LDPE- Recycle	0,938
M4	LDPE- Recycle	0,932
M5	HDPE- Recycle	0,945
M6	HDPE- Recycle	0,944
M7	HDPE- Recycle	0,950
M8	HDPE- Recycle	0,937
M9	LDPE- Recycle	0,956
M10	LDPE- Recycle	0,928
M11	LDPE-RAW	0,920

4.2. Test Amounts

In the analyses, first the seeds and polyethylene materials were subjected to pyrolysis separately. Then, for further testing, the seeds and catalyst materials were mixed to create a composite product. In total, 18 different samples were tested and the experiments were repeated three times at 600, 500, and 400 °C. Test samples are numbered N1 to N18. Analysis weights of seed and catalyst materials and their associated test temperatures are shown in Table 4.3.

Table 4.3. Analysis Test Groups

Test No	Test Heat (^oC)	Sample Amount (gr)
N1	600	50 gr (Seed)
N2	600	25 gr. (M2)
N3	600	25 gr (M11)
N4	600	25 gr (Seed) + 25 gr (M7)
N5	600	25 gr (M7)
N6	600	20 gr (Seed) + 20 gr (M1)
N7	600	20 gr (Seed) + 20 gr (M11)
N8	600	50 gr (Seed)
N9	600	20 gr (Seed) + 20 gr (M10)
N10	600	20 gr (Seed) + 20 gr (M4)
N11	600	20 gr (Seed) + 20 gr (M3)
N12	600	17 gr (Seed) + 17 gr (M6)
N13	600	20 gr (Seed) + 20 gr (M5)
N14	600	14 gr (Seed) + 14 gr (M2)
N15	600	10 gr (Seed) + 10 gr (M2)
N16	500	20 gr (Seed)
N17	500	25 gr (Seed) + 25 gr (M7)
N18	400	25 gr (Seed) + 25 gr (M7)

While creating the test groups, MFI and density values were calculated very closely and PE groups with similar characteristics were analyzed one by one during the test.

Pyrolysis analysis was applied to 18 test groups separately, and the pyrolysis analysis results are given in Table 4.4. The amounts of gas obtained after the analysis were determined according to the ratio of the solid + liquid amounts remaining in the system.

Table 4.4. Pyrolysis Analysis Results

Test No	Amount of Solid+Liquid After Test (gr)	Gas Amount After Test (gr)
N1	17	33
N2	20	5
N3	20	5
N4	9	41
N5	7	22
N6	11	29
N7	17	23
N8	28	22
N9	21	19
N10	13	27
N11	16	24
N12	24	10
N13	26	14
N14	12	16
N15	8	12
N16	8	12
N17	13	37
N18	14	36

4.3. Samples After Pyrolysis

Images of the samples after the pyrolysis experiment are given below according to the test number.

Figure 4.1. Image after N1 Pyrolysis

Figure 4.2. Image after N2 Pyrolysis

Figure 4.3. Image after N3 Pyrolysis

Figure 4.4. Image after N4 Pyrolysis

Figure 4.5. Image after N5 Pyrolysis

Figure 4.6. Image after N6 Pyrolysis

Figure 4.7. Image after N7 Pyrolysis

Figure 4.8. Image after N8 Pyrolysis

Figure 4.9. Image after N9 Pyrolysis

Figure 4.10. Image after N10 Pyrolysis

Figure 4.11. Image after N11 Pyrolysis

Figure 4.12. Image after N12 Pyrolysis

Figure 4.13. Image after N13 Pyrolysis

Figure 4.14. Image after N14 Pyrolysis

Figure 4.15. Image after N15 Pyrolysis

Figure 4.16. Image after N16 Pyrolysis

Figure 4.17. Image after N17 Pyrolysis

Figure 4.18. Image after N18 Pyrolysis

4.4. GC Analysis Results

The gases released during the pyrolysis experiment were taken into gas sample bags. Gases taken into gas sample bags were analyzed with a GC device. The graphical and numerical results of the GC device analysis results are shown below, and the amount of product used in the analysis, temperature values and test results are given in Table 4.5.

According to pyrolysis test results; 19.13%, 21.28%, 38.44% and 63.17% CH_4 gas was obtained from N5, N6, N8 and N16 test samples, respectively. Considering the analysis results, 61.36%, 23.69%, 42.06% and 70.77% H_2 gas was obtained from N5, N6, N8 and N18 test samples, respectively. As the temperature increases in the pyrolysis method, the charring of the product also increases. Temperature monitoring varies depending on the result desired from the product. Depending on which products are desired to be obtained, the temperature is determined experimentally and the experiment is continued. While low temperatures cause water formation, high temperatures cause carbonization in solid waste. At high temperatures, gases volatilize away from the environment and liquids begin to turn tarry.

The release of 100% CO_2 in sample N1 indicated that complete combustion occurred during pyrolysis. Gas groups that cannot be identified by the GC device are stated in the test results as "Other Gases".

Table 4.5. GC Analysis Results

Analiz No	**CH_4 %**	**CO_2 %**	**H_2 %**
N1	**-**	**100**	**-**
N2	No Gas Output Visible		
N3	No Gas Output Visible		
N4	Other Gases		
N5	**19,13**	**19,51**	**61,36**
N6	**21,28**	**55,03**	**23,69**
N7	Other Gases		
N8	**38,44**	**19,5**	**42,06**
N9	Other Gases		
N10	Other Gases		
N11	Other Gases		
N12	Other Gases		
N13	Other Gases		
N14	Other Gases		
N15	Other Gases		
N16	**63,17**	**36,83**	**-**
N17	Other Gases		
N18	**-**	**29,23**	**70,77**

GC device analysis results were added to the study with the device's own outputs. The results are given below, respectively, according to the test results between N1-N18.

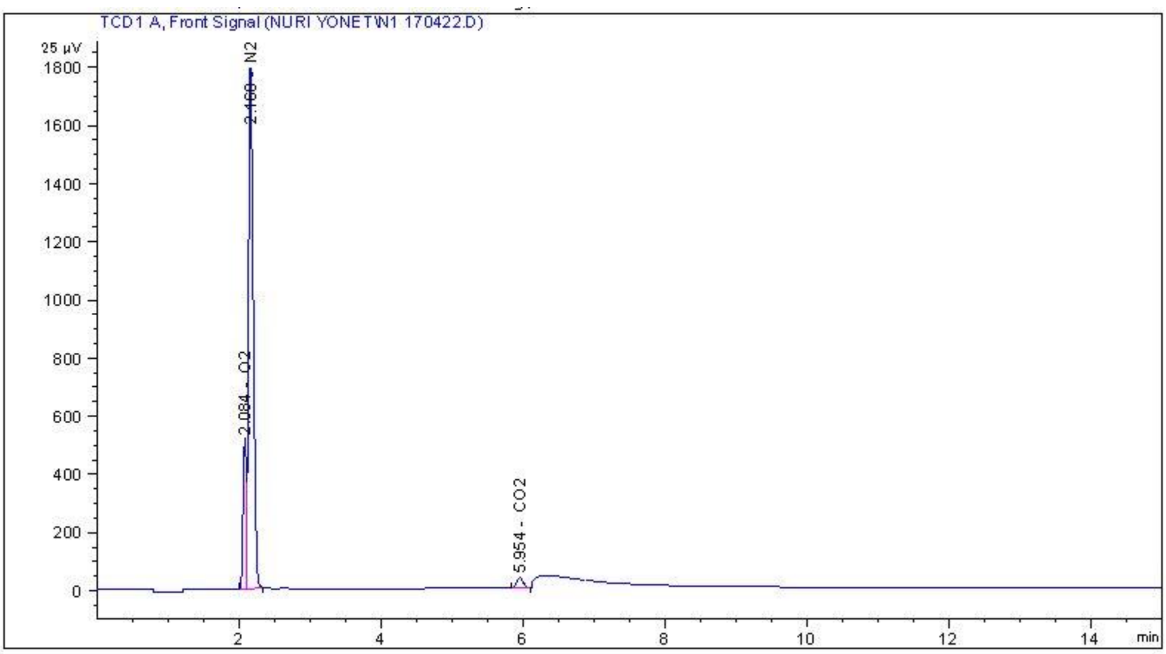

Figure 4.19. N1 GC Analysis Result

Normalized Percent Report

Sorted By : Signal
Calib. Data Modified : 4/19/2022 2:47:52 PM
Multiplier: : 1.0000
Dilution: : 1.0000
Use Multiplier & Dilution Factor with ISTDs

Signal 1: TCD1 A, Front Signal

RetTime [min]	Type	Area [25 µV*s]	Amt/Area	Norm %	Grp	Name
1.006		-	-	-		H2
2.084	BV	1606.69177	0.00000	0.000000		O2
2.160	VB	8162.09082	0.00000	0.000000		N2
2.644		-	-	-		CO
4.440		-	-	-		CH4
5.954	BV	231.61211	4.17464e-3	100.000000		CO2
Totals :				100.000000		

Figure 4.20. N1 GC Analysis Numerical Result

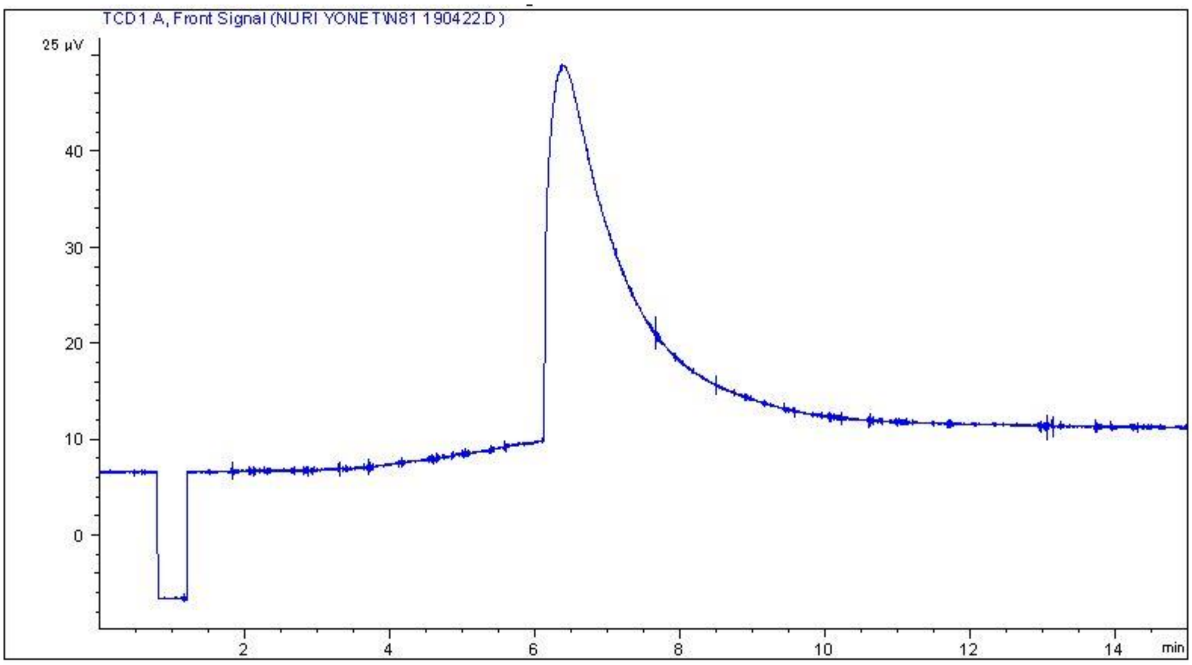

Figure 4.21. N2 GC Analysis Result

Normalized Percent Report

===

Sorted By : Signal
Calib. Data Modified : 4/19/2022 2:47:52 PM
Multiplier: : 1.0000
Dilution: : 1.0000
Use Multiplier & Dilution Factor with ISTDs

Signal 1: TCD1 A, Front Signal

RetTime [min]	Type	Area [25 µV*s]	Amt/Area	Norm %	Grp	Name
1.006		-	-	-		H2
2.101		-	-	-		O2
2.107		-	-	-		N2
2.644		-	-	-		CO
4.440		-	-	-		CH4
6.031		-	-	-		CO2

Totals : 0.000000

Figure 4.22. N2 GC Analysis Numerical Result

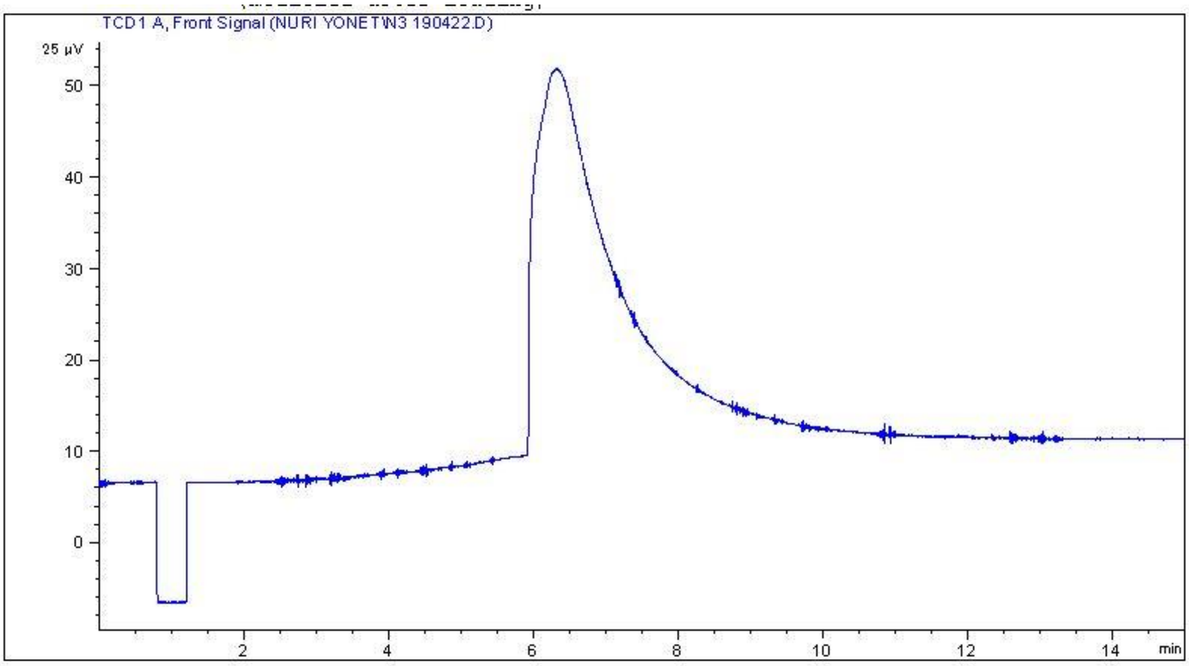

Figure 4.23. N3 GC Analysis Result

```
                          Normalized Percent Report
=====================================================================

Sorted By              :       Signal
Calib. Data Modified   :       4/19/2022 2:47:52 PM
Multiplier:                     :       1.0000
Dilution:                       :       1.0000
Use Multiplier & Dilution Factor with ISTDs

Signal 1: TCD1 A, Front Signal

RetTime  Type     Area      Amt/Area      Norm     Grp   Name
 [min]          [25 µV*s]                  %
-------|------|----------|----------|----------|--|------------------
  1.006            -          -          -           H2
  2.101            -          -          -           O2
  2.107            -          -          -           N2
  2.644            -          -          -           CO
  4.440            -          -          -           CH4
  6.031            -          -          -           CO2

Totals :                                0.000000
```

Figure 4.24. N3 GC Analysis Numerical Result

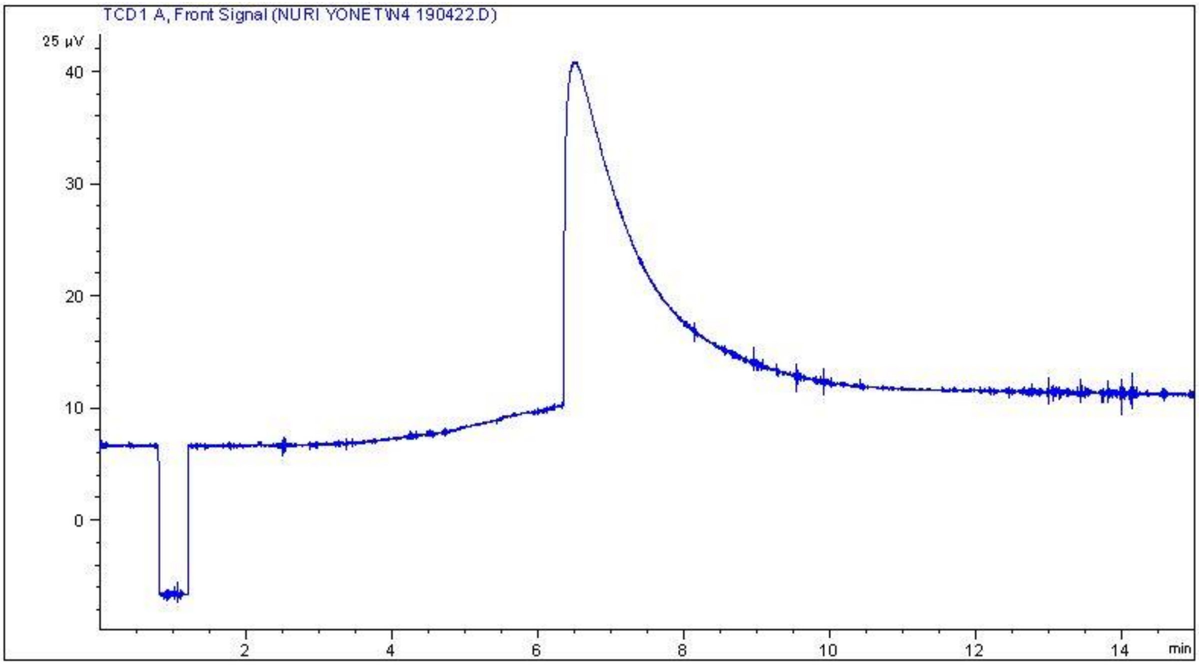

Figure 4.25. N4 GC Analysis Result

Normalized Percent Report

===

Sorted By : Signal
Calib. Data Modified : 4/19/2022 2:47:52 PM
Multiplier: : 1.0000
Dilution: : 1.0000
Use Multiplier & Dilution Factor with ISTDs

Signal 1: TCD1 A, Front Signal

RetTime [min]	Type	Area [25 µV*s]	Amt/Area	Norm %	Grp	Name
1.006		-	-	-		H2
2.101		-	-	-		O2
2.107		-	-	-		N2
2.644		-	-	-		CO
4.440		-	-	-		CH4
6.031		-	-	-		CO2

Totals : 0.000000

Figure 4.26. N4 GC Analysis Numerical Result

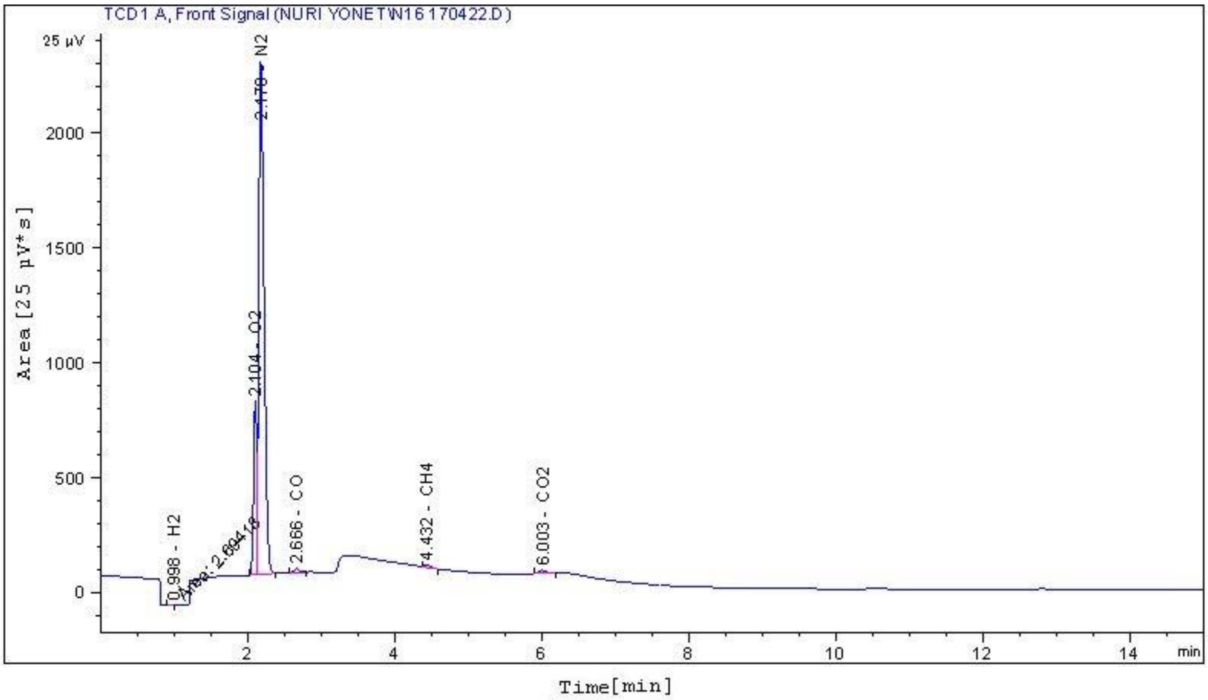

Figure 4.27. N5 GC Analysis Result

Normalized Percent Report

===

Sorted By : Signal
Calib. Data Modified : 4/17/2022 10:18:56 PM
Multiplier: : 1.0000
Dilution: : 1.0000
Use Multiplier & Dilution Factor with ISTDs

Signal 1: TCD1 A, Front Signal

RetTime [min]	Type	Area [25 µV*s]	Amt/Area	Norm %	Grp	Name
0.998	MM	2.69418	3.77733e-1	61.357020		H2
2.104	BV	2332.88696	0.00000	0.000000		O2
2.178	VB	1.07530e4	0.00000	0.000000		N2
2.666	BB	80.81384	0.00000	0.000000		CO
4.432	BB	56.93528	5.57356e-3	19.132314		CH4
6.003	BB	77.51758	4.17464e-3	19.510666		CO2

Totals : 100.000000

Figure 4.28. N5 GC Analysis Numerical Result

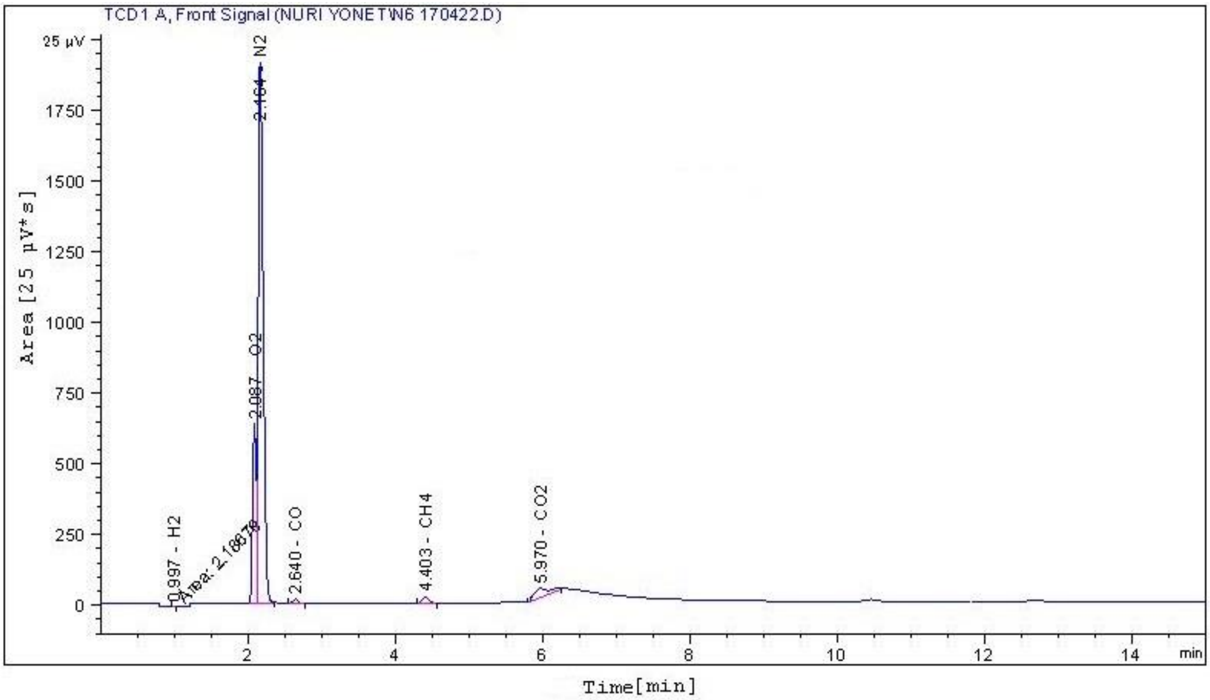

Figure 4.29. N6 GC Analysis Result

Normalized Percent Report

==

Sorted By : Signal
Calib. Data Modified : 4/17/2022 10:39:36 PM
Multiplier: : 1.0000
Dilution: : 1.0000
Use Multiplier & Dilution Factor with ISTDs

Signal 1: TCD1 A, Front Signal

RetTime [min]	Type	Area [25 µV*s]	Amt/Area	Norm %	Grp	Name
0.997	MM	2.18679	3.77733e-1	23.687538		H2
2.087	BV	1993.27271	0.00000	0.000000		O2
2.164	VB	8884.88574	0.00000	0.000000		N2
2.640	BB	63.23287	0.00000	0.000000		CO
4.403	BB	133.13766	5.57356e-3	21.279522		CH4
5.970	BB	459.70151	4.17464e-3	55.032940		CO2

Totals : 100.000000

Figure 4.30. N6 GC Analysis Numerical Result

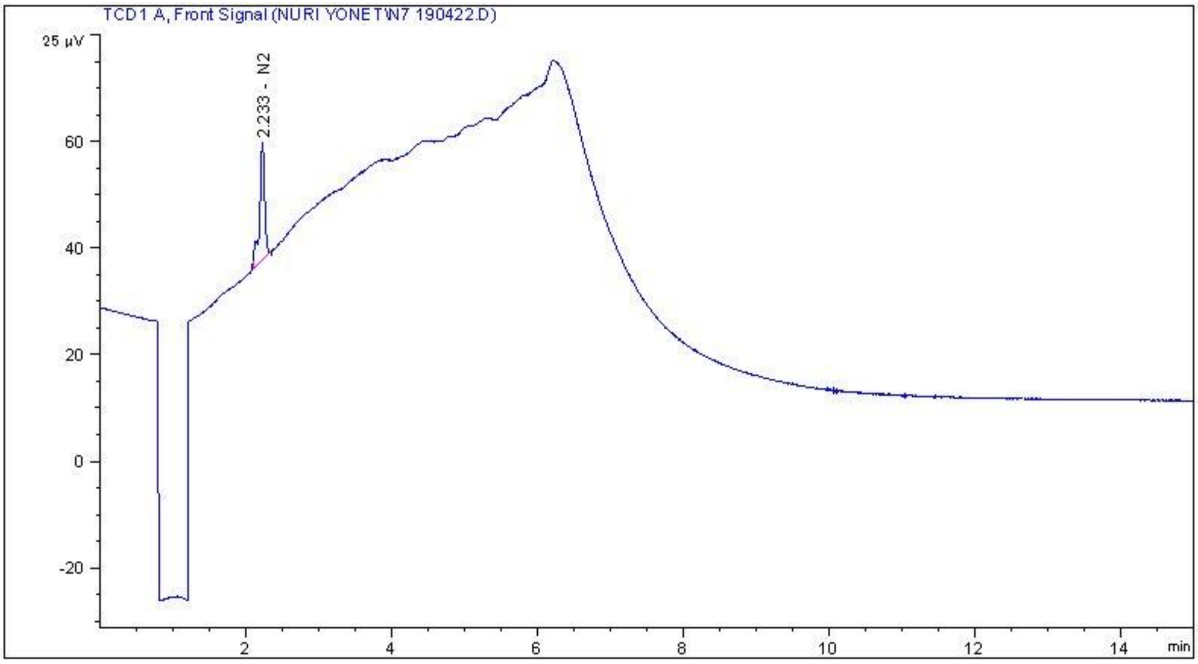

Figure 4.31. N7 GC Analysis Result

Normalized Percent Report

==

Sorted By : Signal
Calib. Data Modified : 4/19/2022 2:47:52 PM
Multiplier: : 1.0000
Dilution: : 1.0000
Use Multiplier & Dilution Factor with ISTDs

Signal 1: TCD1 A, Front Signal

RetTime [min]	Type	Area [25 µV*s]	Amt/Area	Norm %	Grp	Name
1.006		-	-	-		H2
2.101		-	-	-		O2
2.233	BB	107.89826	0.00000	0.000000		N2
2.644		-	-	-		CO
4.440		-	-	-		CH4
6.031		-	-	-		CO2

Totals : 0.000000

Figure 4.32. N7 GC Analysis Numerical Result

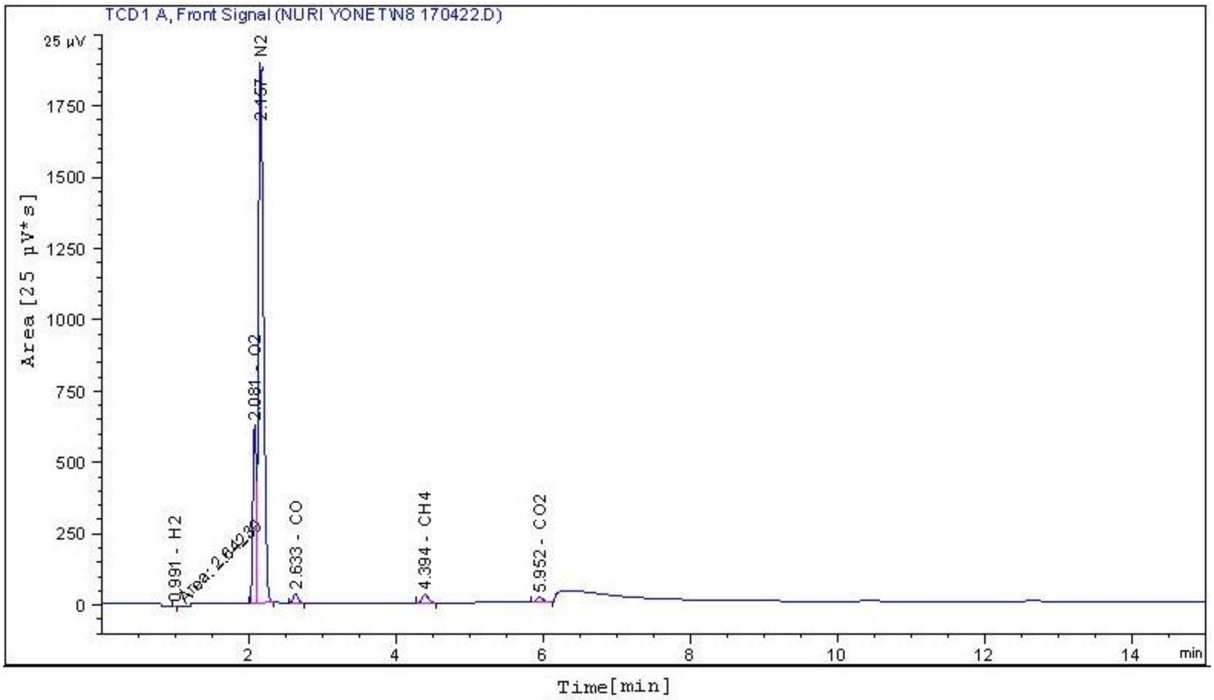

Figure 4.33. N8 GC Analysis Result

Normalized Percent Report

==

Sorted By : Signal
Calib. Data Modified : 4/17/2022 10:39:36 PM
Multiplier: : 1.0000
Dilution: : 1.0000
Use Multiplier & Dilution Factor with ISTDs

Signal 1: TCD1 A, Front Signal

RetTime [min]	Type	Area [25 µV*s]	Amt/Area	Norm %	Grp	Name
0.991	MM	2.64239	3.77733e-1	42.058795		H2
2.081	BV	1966.67004	0.00000	0.000000		O2
2.157	VB	8757.80078	0.00000	0.000000		N2
2.633	BB	146.64096	0.00000	0.000000		CO
4.394	BB	163.68353	5.57356e-3	38.442570		CH4
5.952	BV	110.84368	4.17464e-3	19.498635		CO2

Totals : 100.000000

Figure 4.34. N8 GC Analysis Numerical Result

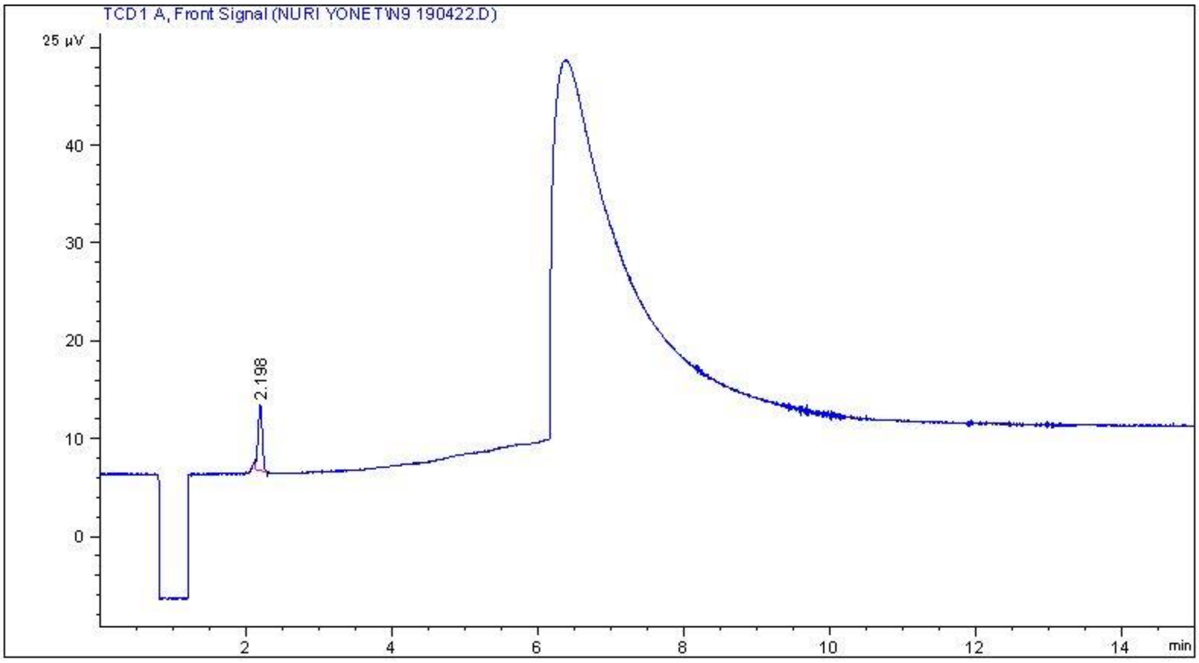

Figure 4.35. N9 GC Analysis Result

Normalized Percent Report

==

Sorted By : Signal
Calib. Data Modified : Wednesday, December 15, 2021 12:15:05 PM
Multiplier: : 1.0000
Dilution: : 1.0000
Use Multiplier & Dilution Factor with ISTDs

Signal 1: TCD1 A, Front Signal

RetTime [min]	Type	Area [25 µV*s]	Amt/Area	Norm %	Grp	Name
1.006		-	-	-		H2
4.440		-	-	-		CH4
6.031		-	-	-		CO2

Totals : 0.000000

Figure 4.36. N9 GC Analysis Numerical Result

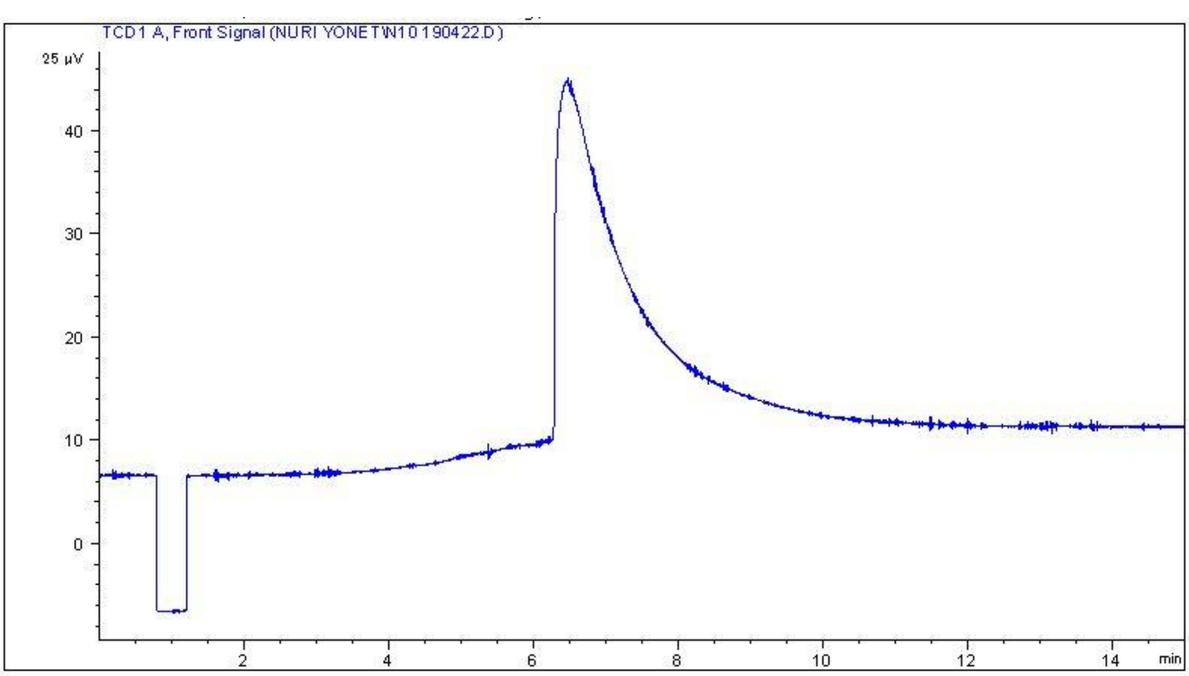

Figure 4.37. N10 GC Analysis Result

```
                    Normalized Percent Report
=====================================================================

Sorted By                 :      Signal
Calib. Data Modified      :      Wednesday, December 15, 2021 12:15:05 PM
Multiplier:                        :        1.0000
Dilution:                          :        1.0000
Use Multiplier & Dilution Factor with ISTDs

Signal 1: TCD1 A, Front Signal

RetTime  Type     Area      Amt/Area      Norm     Grp   Name
 [min]          [25 µV*s]                  %
-------|------|----------|----------|----------|--|------------------
  1.006            -          -           -          H2
  4.440            -          -           -          CH4
  6.031            -          -           -          CO2

Totals :                                0.000000
```

Figure 4.38. N10 GC Analysis Numerical Result

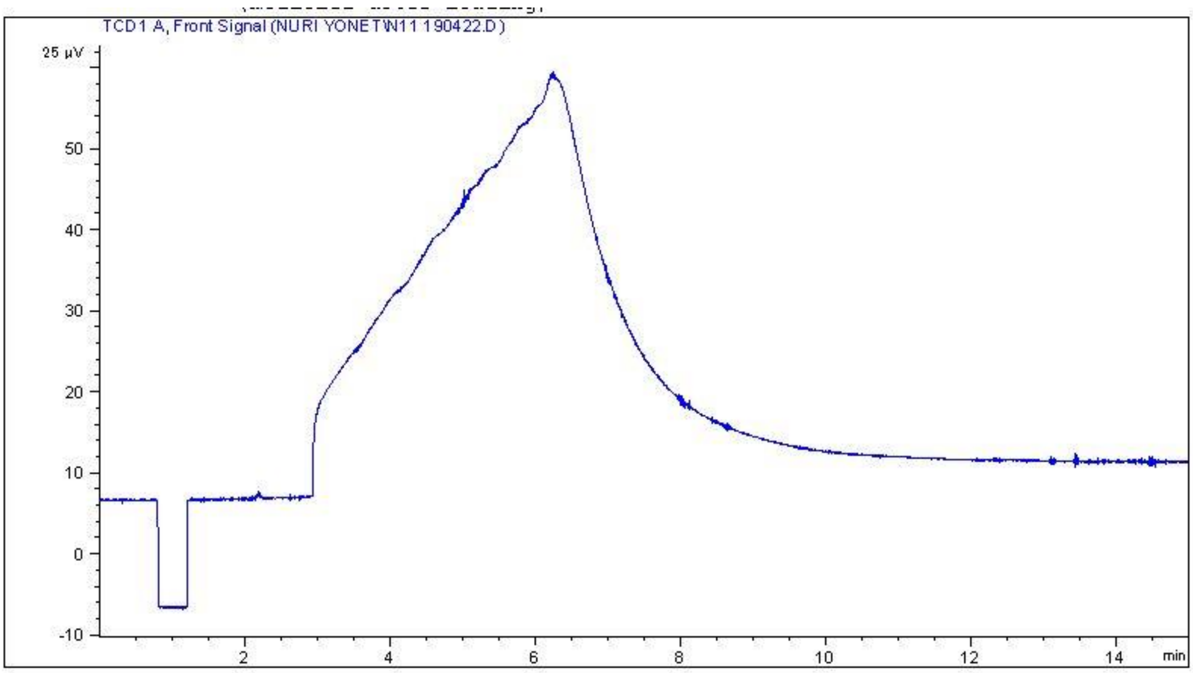

Figure 4.39. N11 GC Analysis Result

Normalized Percent Report

==

Sorted By : Signal
Calib. Data Modified : Wednesday, December 15, 2021 12:15:05 PM
Multiplier: : 1.0000
Dilution: : 1.0000
Use Multiplier & Dilution Factor with ISTDs

Signal 1: TCD1 A, Front Signal

RetTime [min]	Type	Area [25 µV*s]	Amt/Area	Norm %	Grp	Name
1.006		-	-	-		H2
4.440		-	-	-		CH4
6.031		-	-	-		CO2

Totals : 0.000000

Figure 4.40. N11 GC Analysis Numerical Result

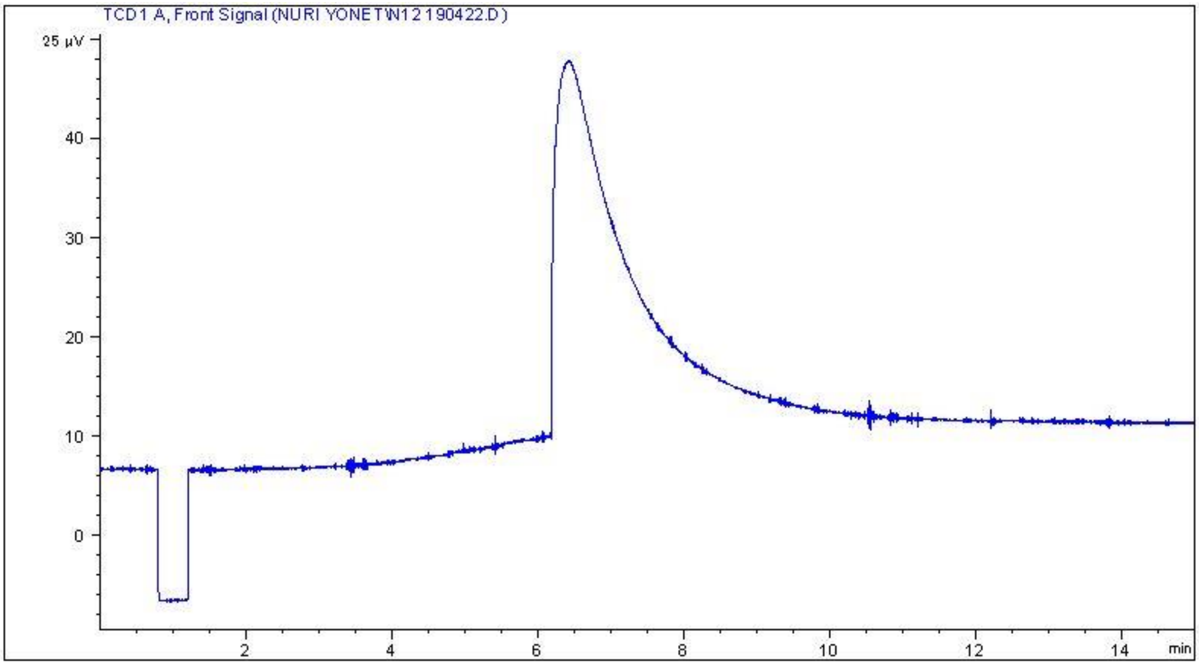

Figure 4.41. N12 GC Analysis Result

Normalized Percent Report

===

Sorted By : Signal
Calib. Data Modified : Wednesday, December 15, 2021 12:15:05 PM
Multiplier: : 1.0000
Dilution: : 1.0000
Use Multiplier & Dilution Factor with ISTDs

Signal 1: TCD1 A, Front Signal

RetTime [min]	Type	Area [25 µV*s]	Amt/Area	Norm %	Grp	Name
1.006		-	-	-		H2
4.440		-	-	-		CH4
6.031		-	-	-		CO2

Totals : 0.000000

Figure 4.42. N12 GC Analysis Numerical Result

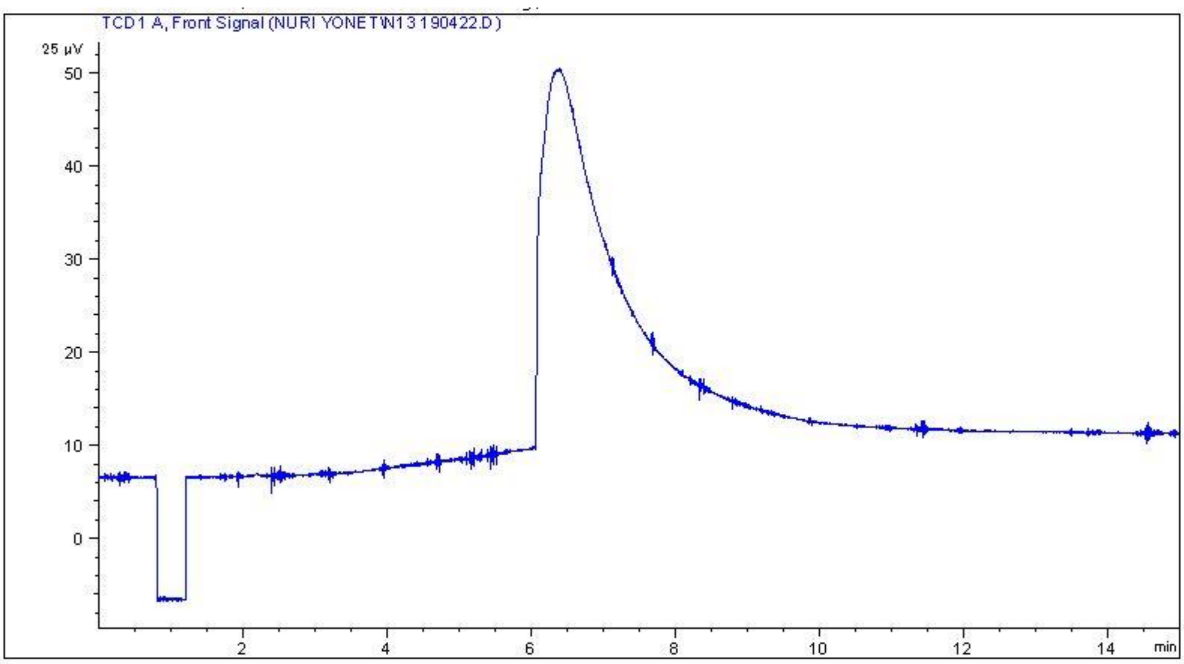

Figure 4.43. N13 GC Analysis Result

Normalized Percent Report

==

Sorted By : Signal
Calib. Data Modified : Wednesday, December 15, 2021 12:15:05 PM
Multiplier: : 1.0000
Dilution: : 1.0000
Use Multiplier & Dilution Factor with ISTDs

Signal 1: TCD1 A, Front Signal

RetTime [min]	Type	Area [25 µV*s]	Amt/Area	Norm %	Grp	Name
1.006		-	-	-		H2
4.440		-	-	-		CH4
6.031		-	-	-		CO2

Totals : 0.000000

Figure 4.44. N13 GC Analysis Numerical Result

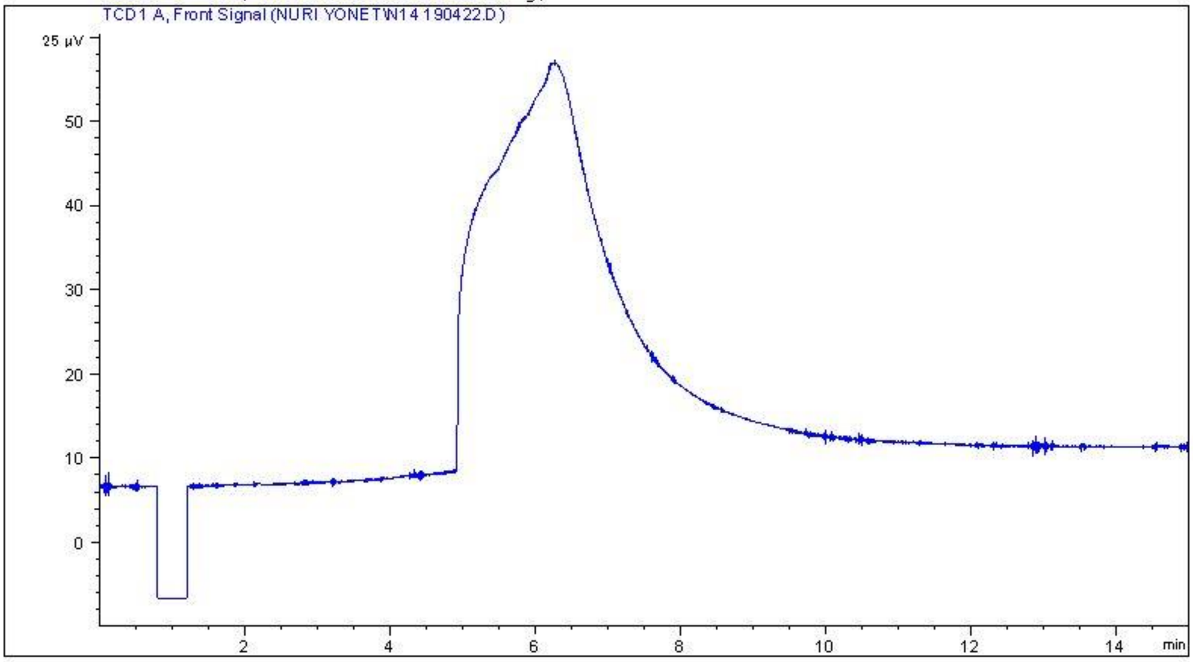

Figure 4.45. N14 GC Analysis Result

```
                       Normalized Percent Report
======================================================================

Sorted By              :      Signal
Calib. Data Modified   :      Wednesday, December 15, 2021 12:15:05 PM
Multiplier:                    :      1.0000
Dilution:                      :      1.0000
Use Multiplier & Dilution Factor with ISTDs

Signal 1: TCD1 A, Front Signal

RetTime  Type     Area      Amt/Area      Norm     Grp   Name
 [min]          [25 µV*s]                  %
-------|------|----------|----------|----------|--|------------------
  1.006            -          -          -          H2
  4.440            -          -          -          CH4
  6.031            -          -          -          CO2

Totals :                                0.000000
```

Figure 4.46. N14 GC Analysis Numerical Result

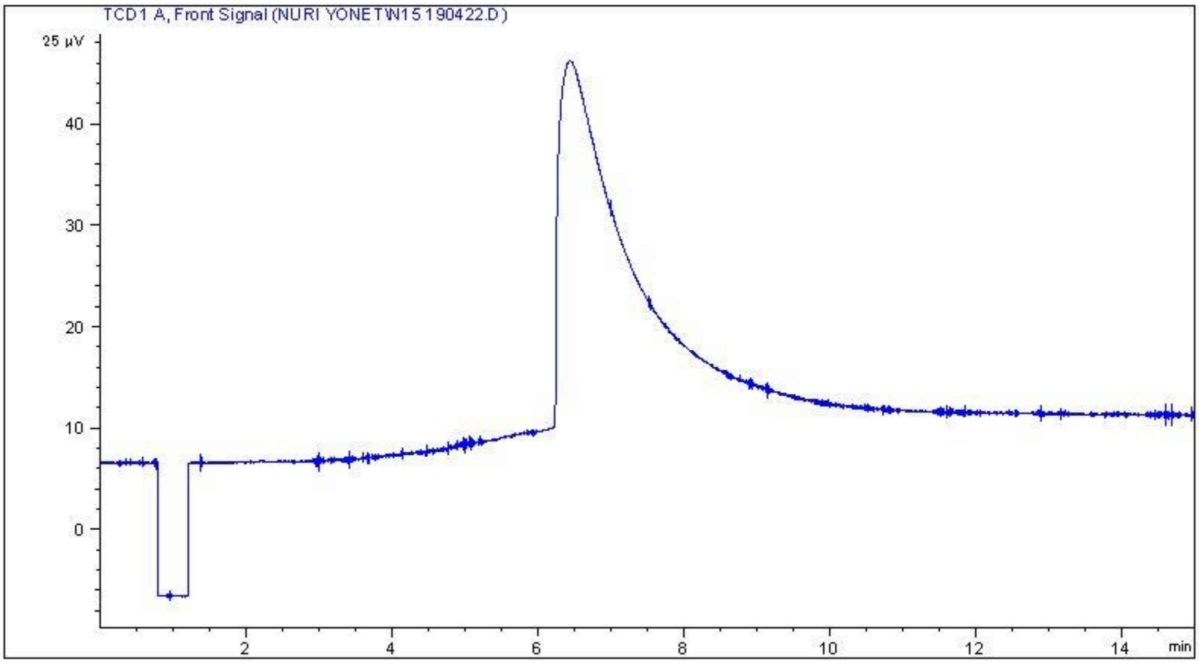

Figure 4.47. N15 GC Analysis Result

==

Normalized Percent Report

==

Sorted By : Signal
Calib. Data Modified : Wednesday, December 15, 2021 12:15:05 PM
Multiplier: : 1.0000
Dilution: : 1.0000
Use Multiplier & Dilution Factor with ISTDs

Signal 1: TCD1 A, Front Signal

RetTime [min]	Type	Area [25 µV*s]	Amt/Area	Norm %	Grp	Name
1.006		-	-	-		H2
4.440		-	-	-		CH4
6.031		-	-	-		CO2

Totals : 0.000000

Figure 4.48. N15 GC Analysis Numerical Result

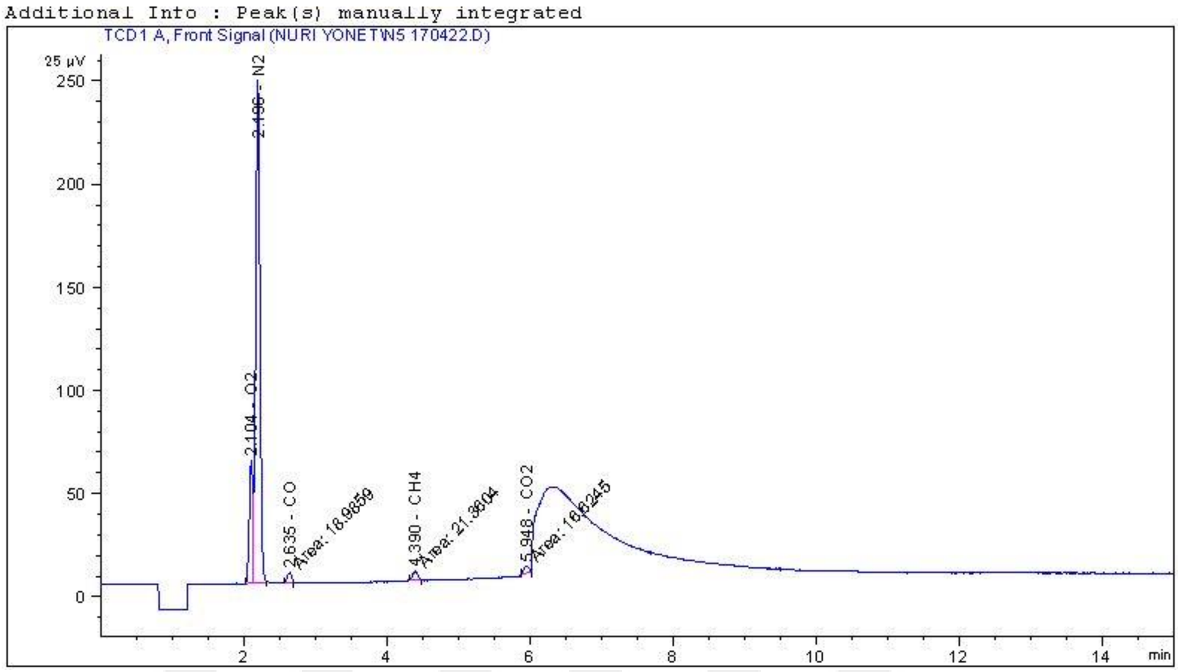

Figure 4.49. N16 GC Analysis Result

```
=====================================================================
                      Normalized Percent Report
=====================================================================

Sorted By                 :      Signal
Calib. Data Modified      :      4/17/2022 10:39:36 PM
Multiplier:                        :       1.0000
Dilution:                          :       1.0000
Use Multiplier & Dilution Factor with ISTDs

Signal 1: TCD1 A, Front Signal

RetTime  Type     Area      Amt/Area      Norm     Grp   Name
 [min]          [25 µV*s]                   %
-------|------|----------|----------|----------|--|------------------
  1.006            -           -           -          H2
  2.104 BV     204.68608    0.00000    0.000000       O2
  2.196 VB    1008.89941    0.00000    0.000000       N2
  2.635 MM      18.98595    0.00000    0.000000       CO
  4.390 MM      21.36040 5.57356e-3   63.173499       CH4
  5.948 MM      16.62452 4.17464e-3   36.826501       CO2

Totals :                              100.000000
```

Figure 4.50. N16 GC Analysis Numerical Result

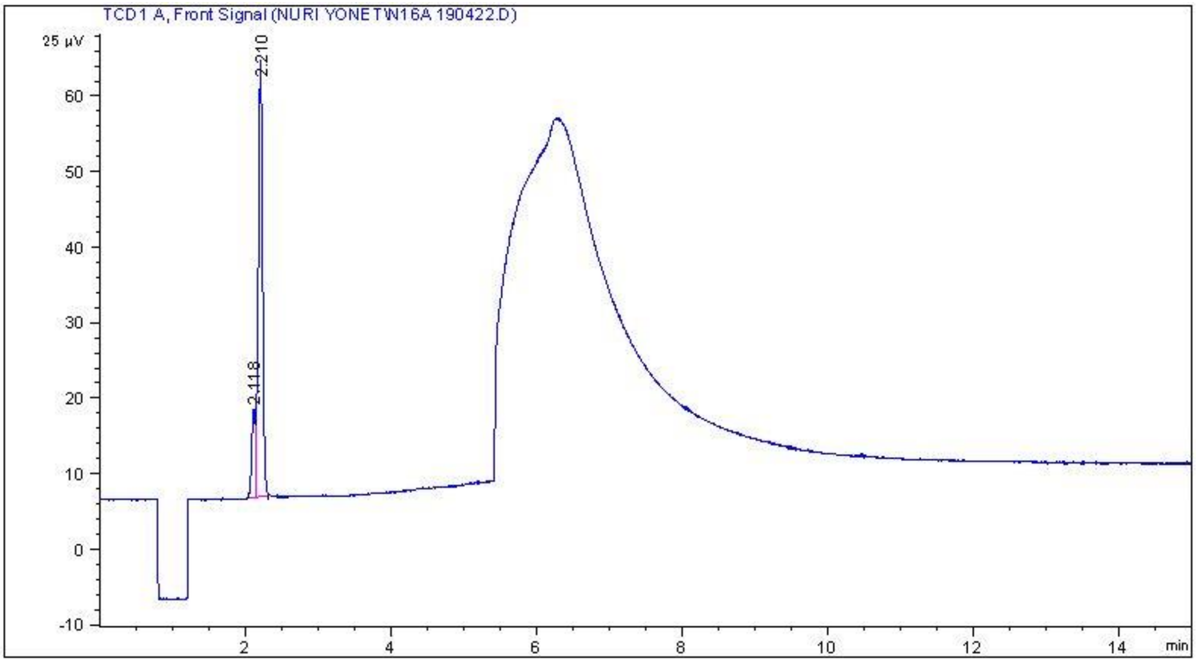

Figure 4.51. N17 GC Analysis Result

Normalized Percent Report

==

Sorted By : Signal
Calib. Data Modified : Wednesday, December 15, 2021 12:15:05 PM
Multiplier: : 1.0000
Dilution: : 1.0000
Use Multiplier & Dilution Factor with ISTDs

Signal 1: TCD1 A, Front Signal

RetTime [min]	Type	Area [25 µV*s]	Amt/Area	Norm %	Grp	Name
1.006		-	-	-		H2
4.440		-	-	-		CH4
6.031		-	-	-		CO2

Totals : 0.000000

Figure 4.52. N17 GC Analysis Numerical Result

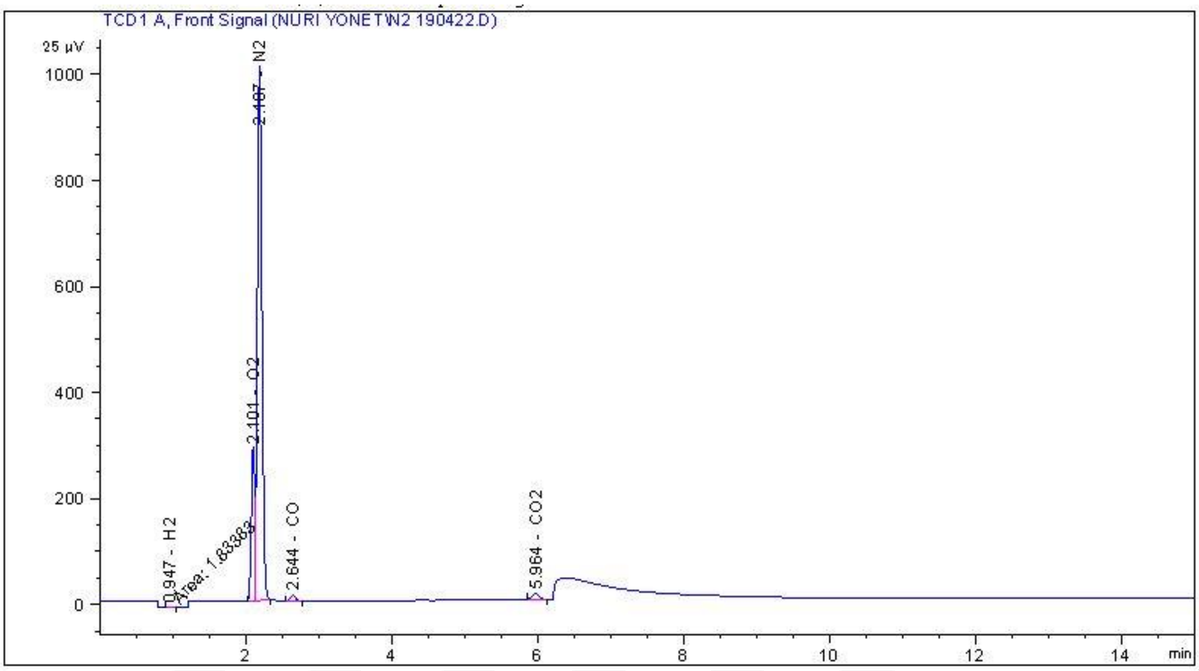

Figure 4.53. N18 GC Analysis Result

Normalized Percent Report

Sorted By : Signal
Calib. Data Modified : 4/19/2022 2:47:52 PM
Multiplier: : 1.0000
Dilution: : 1.0000
Use Multiplier & Dilution Factor with ISTDs

Signal 1: TCD1 A, Front Signal

RetTime [min]	Type	Area [25 µV*s]	Amt/Area	Norm %	Grp	Name
0.947	MM	1.83383	3.77733e-1	70.766877		H2
2.101	BV	964.76593	0.00000	0.000000		O2
2.187	VB	4337.15723	0.00000	0.000000		N2
2.644	BB	50.57015	0.00000	0.000000		CO
4.440		-	-	-		CH4
5.964	BB	68.54405	4.17464e-3	29.233123		CO2
Totals :				100.000000		

Figure 4.54. N18 GC Analysis Numerical Result

Out of 18 samples tested, five sample results gave interpretable results. Other analysis results are samples containing unidentified gases or without gas evolution.

As a result of N18 analysis, 70.77% H_2 gas was obtained. He showed that H_2 gas could be obtained at low temperature, even before pyrolysis was completed. Similar results were observed by Ball et al. (2016), whose sample was heated to 400 °C with a heating rate of 50 °C/min. At 450-500 °C, most of the H_2 gas has moved away from the pyrolysis system [56].

According to the results, the highest CH_4 yield was reached in the N16 sample. In the gas property analysis, it was determined that 63.17% CH_4 was the most suitable gas in terms of flammability and usability instead of natural gas.

The N6 sample was analyzed as a mixture of 50% seed and M1 PE material. It consists of 21.78% CH_4, 55.03% CO_2 and 23.69% H_2. It was observed that with the addition of M1 material, the CH_4 ratio decreased and H_2 gas emerged.

In the analysis of the N8 sample, the seed amount and temperature were analyzed by increasing 100 °C compared to the N16 sample. Increasing the temperature to 600 °C caused the CH_4 ratio to decrease and other gases to form.

Sample N5 contains the seedless catalyst. In order to better see the gas density, the M7 catalyst PE material, which has the highest density and lowest viscosity, was pyrolyzed. As a result of the experiment, 61.36% H_2 gas release was observed.

4.5. Microstructure Results

The surface microstructures of the seeds before pyrolysis were observed. After pyrolysis, the surface roughness of each test sample was checked with an optical microscope to see the carbonization status. The magnification ratio of the microscope was set to X5 or X10. Microscope images of the test samples are given below, respectively.

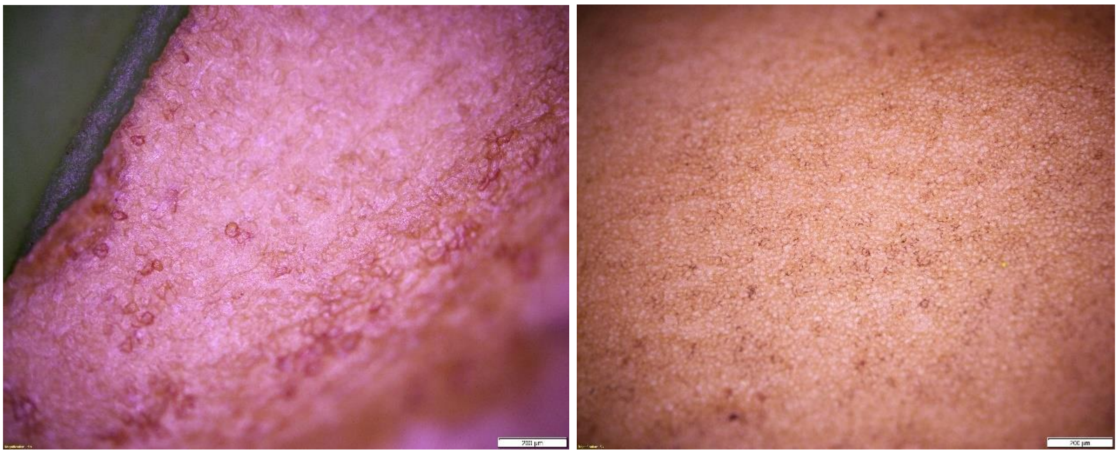

(a) (b)

Figure 4.55. Seed Microstructure Before Pyrolysis

a) Seed Internal Structure b) Seed External Structure

(a) (b)

Figure 4.56. N1 Microstructure After Pyrolysis a) Internal Structure b) External Structure

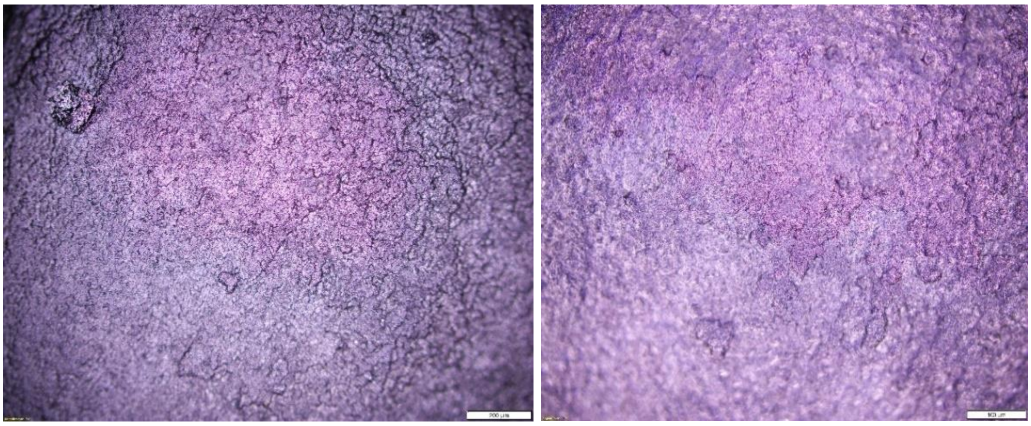

(a) (b)

Figure 4.57. N2 Microstructure After Pyrolysis a) Internal Structure b) External Structure

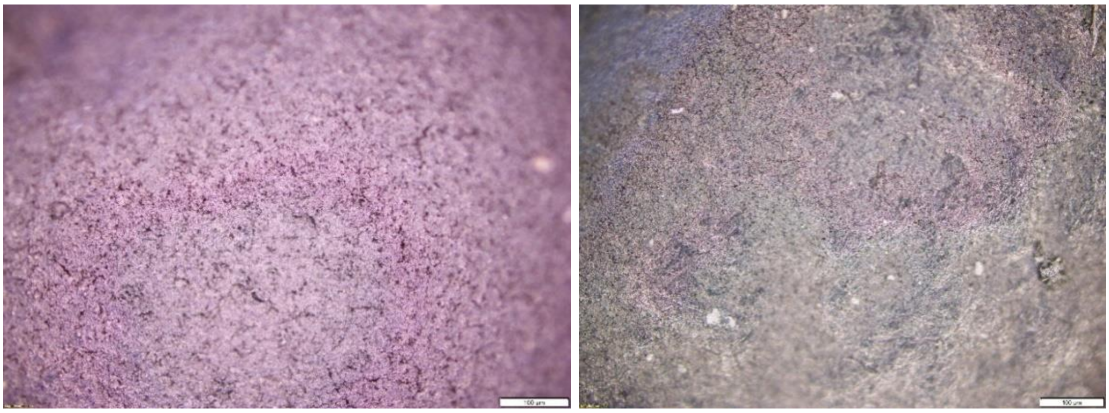

(a) (b)

Figure 4.58. N3 Microstructure After Pyrolysis a) Internal Structure b) External Structure

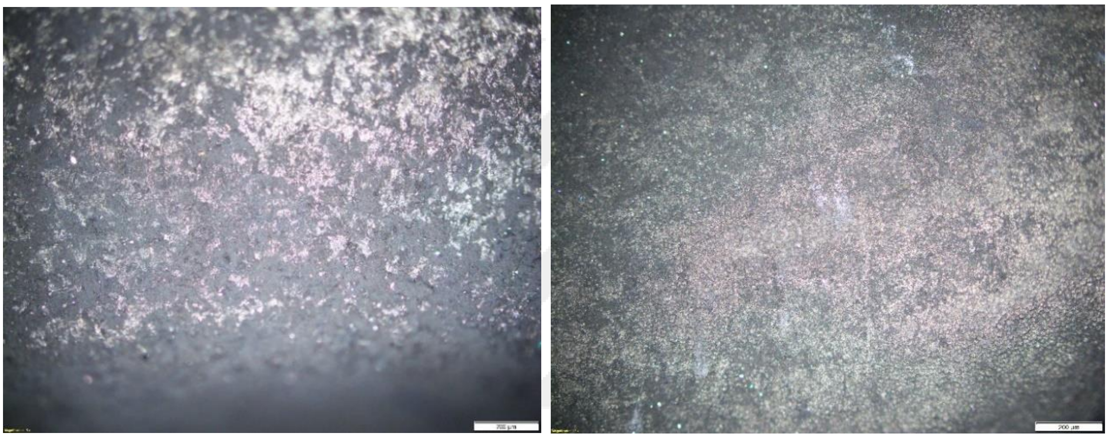

(a) (b)

Figure 4.59. N4 Microstructure After Pyrolysis a) Internal Structure b) External Structure

(a) (b)

Figure 4.60. N5 Microstructure After Pyrolysis a) Internal Structure b) External Structure

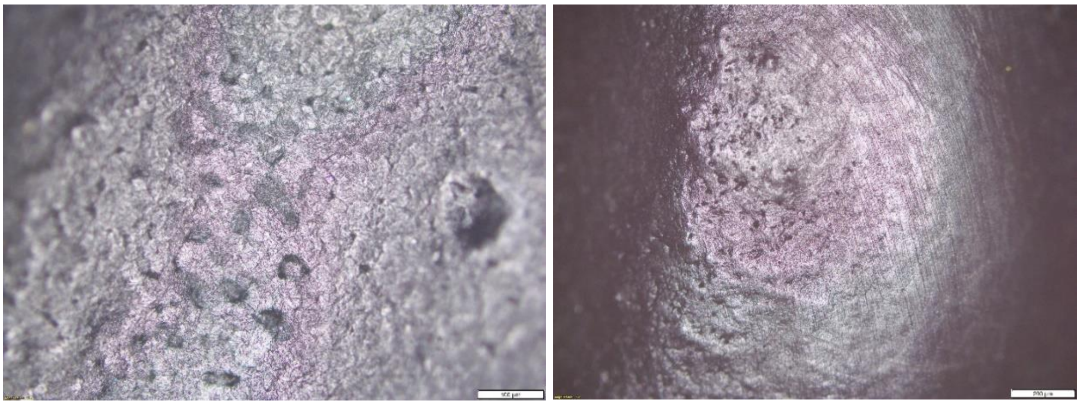

(a) (b)

Figure 4.61. N6 Microstructure After Pyrolysis a) Internal Structure b) External Structure

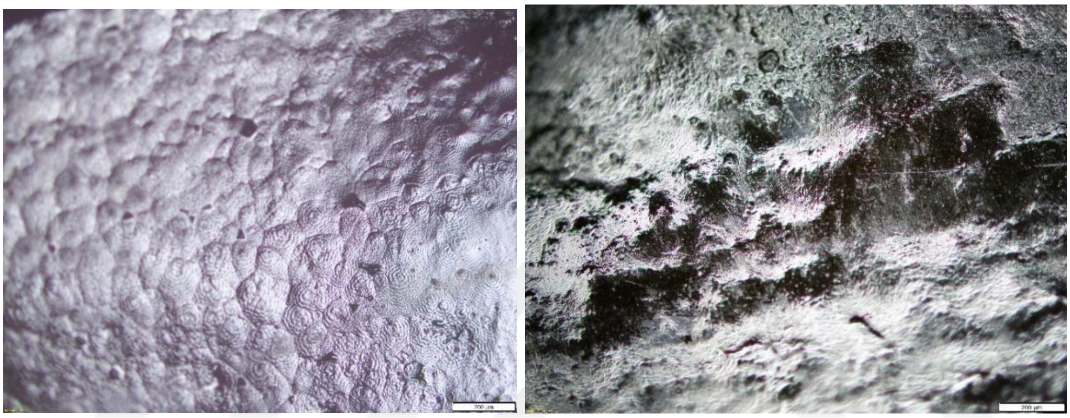

(a) (b)

Figure 4.62. N7 Microstructure After Pyrolysis a) Internal Structure b) External Structure

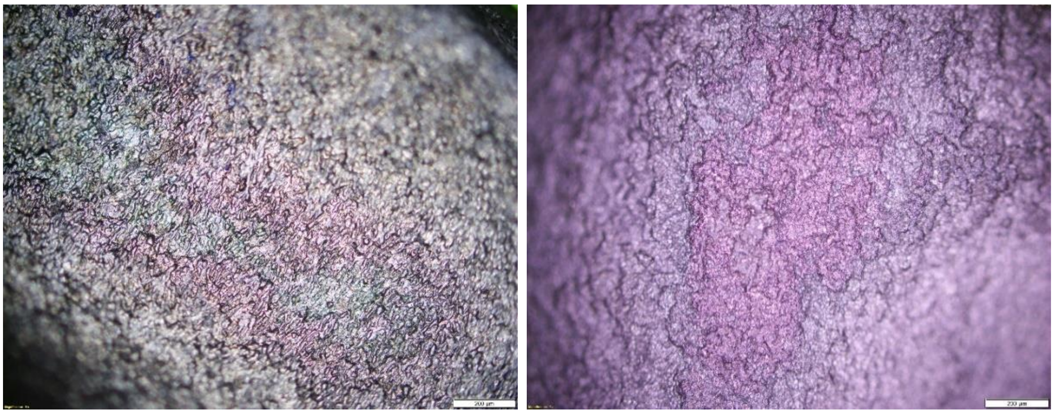

(a) (b)

Figure 4.63. N8 Microstructure After Pyrolysis a) Internal Structure b) External Structure

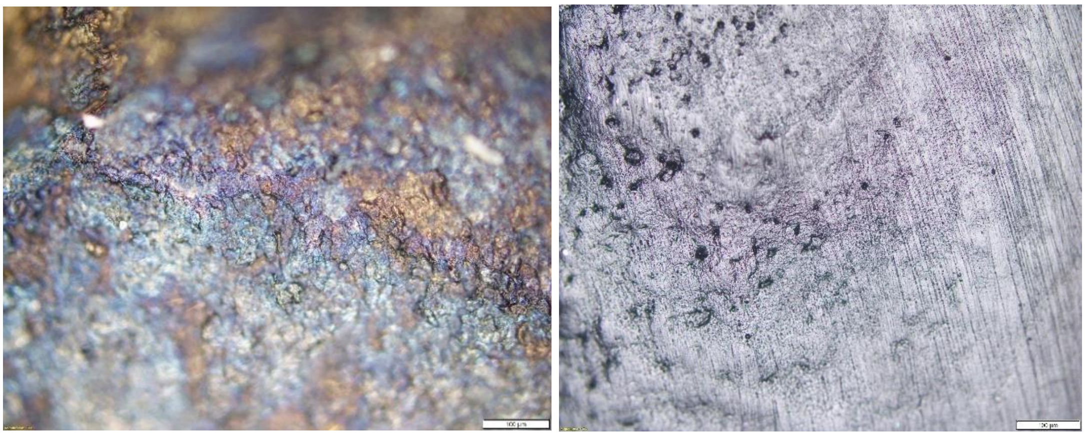

(a) (b)

Figure 4.64. N9 Microstructure After Pyrolysis a) Internal Structure b) External Structure

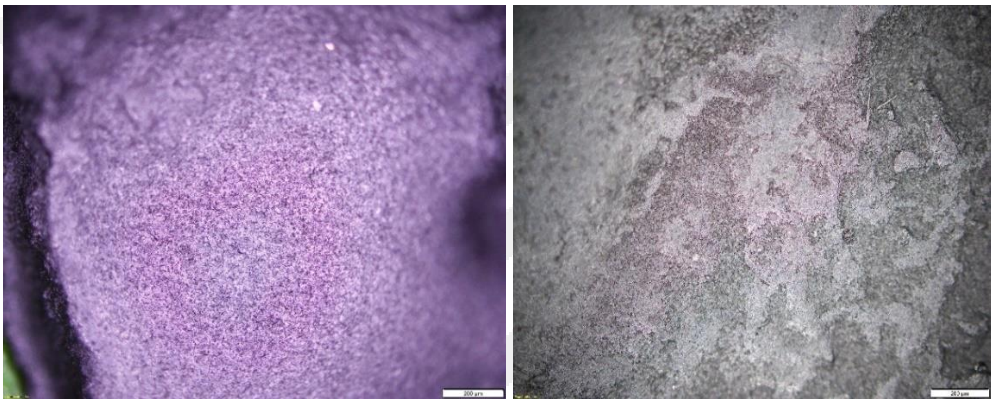

(a) (b)

Figure 4.65. N10 Microstructure After Pyrolysis a) Internal Structure b) External Structure

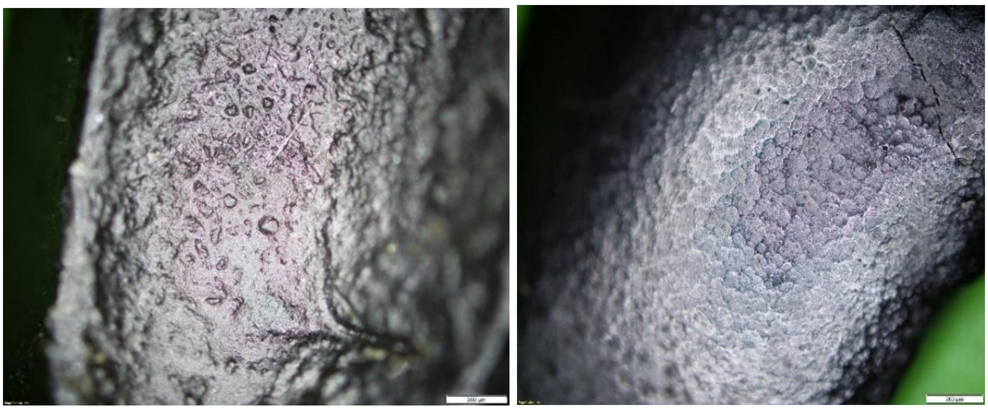

(a) (b)

Figure 4.66. 11 Microstructure After Pyrolysis a) Internal Structure b) External Structure

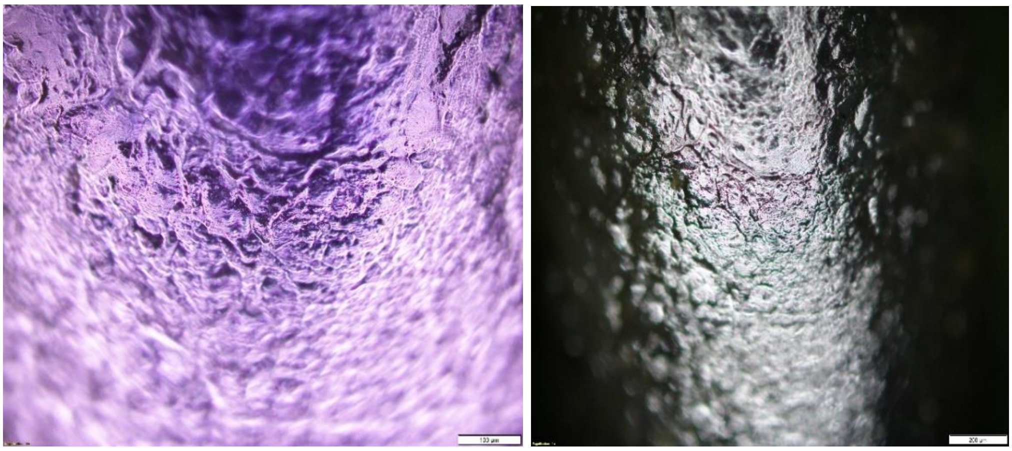

(a) (b)

Figure 4.67. N12 Microstructure After Pyrolysis a) Internal Structure b) External Structure

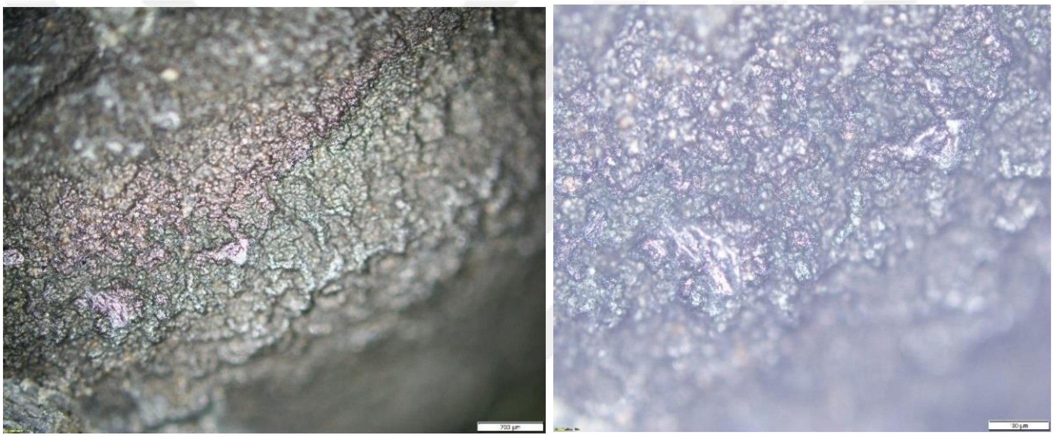

(a) (b)

Figure 4.68. N13 Microstructure After Pyrolysis a) Internal Structure b) External Structure

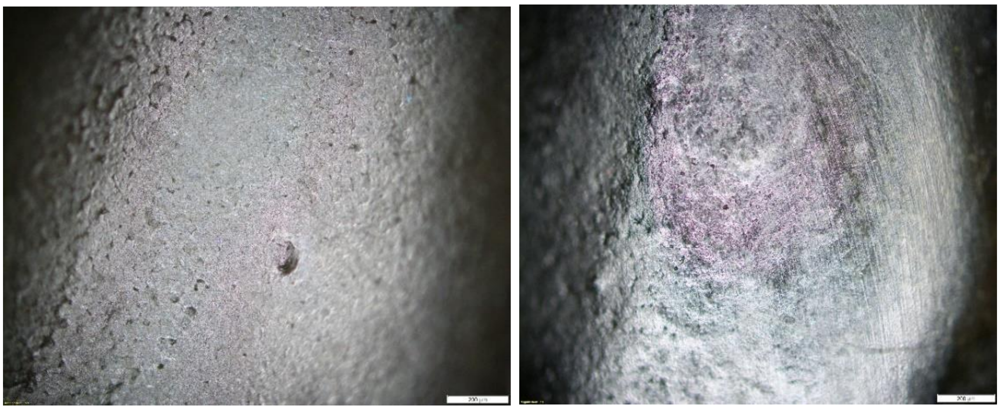

(a) (b)

Figure 4.69. N14 Microstructure After Pyrolysis a) Internal Structure b) External Structure

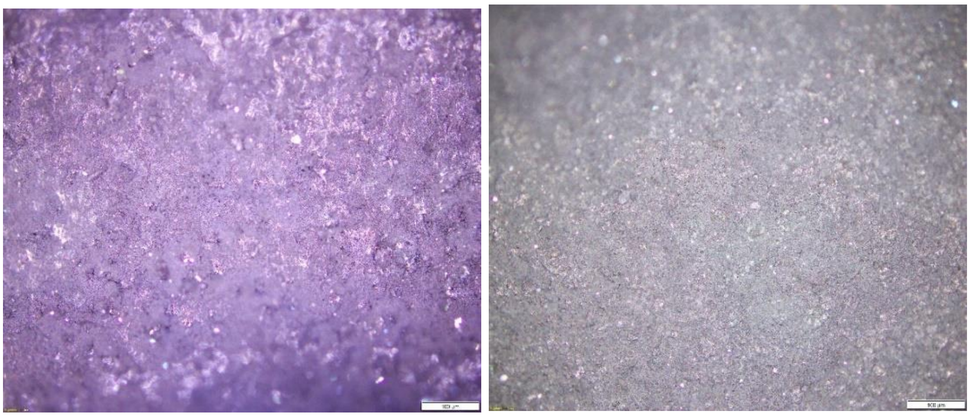

(a) (b)

Figure 4.70. N15 Microstructure After Pyrolysis a) Internal Structure b) External Structure

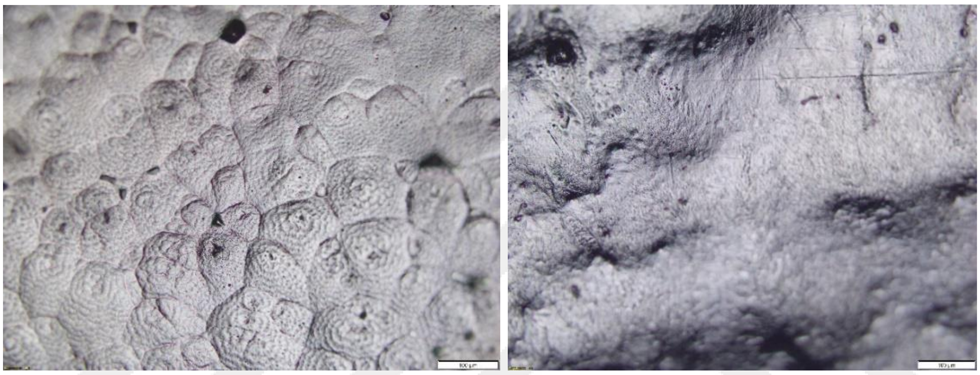

(a) (b)

Figure 4.71. N16 Microstructure After Pyrolysis a) Internal Structure b) External Structure

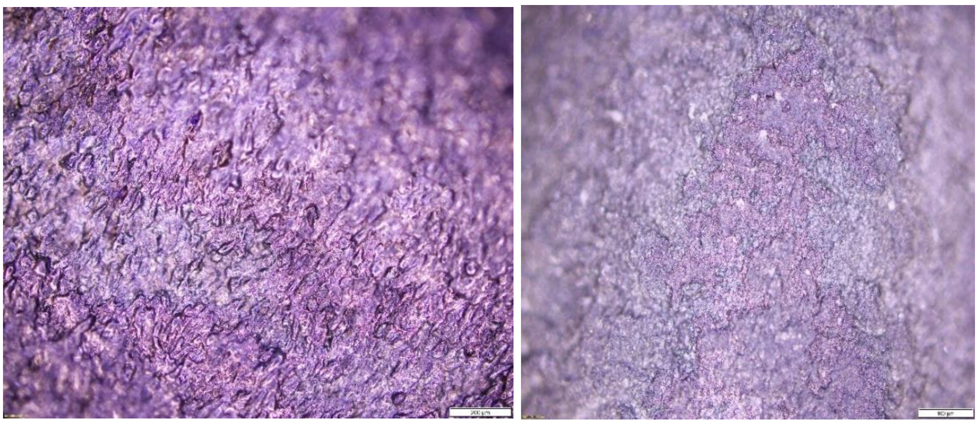

(a) (b)

Figure 4.72. N17 Microstructure After Pyrolysis a) Internal Structure b) External Structure

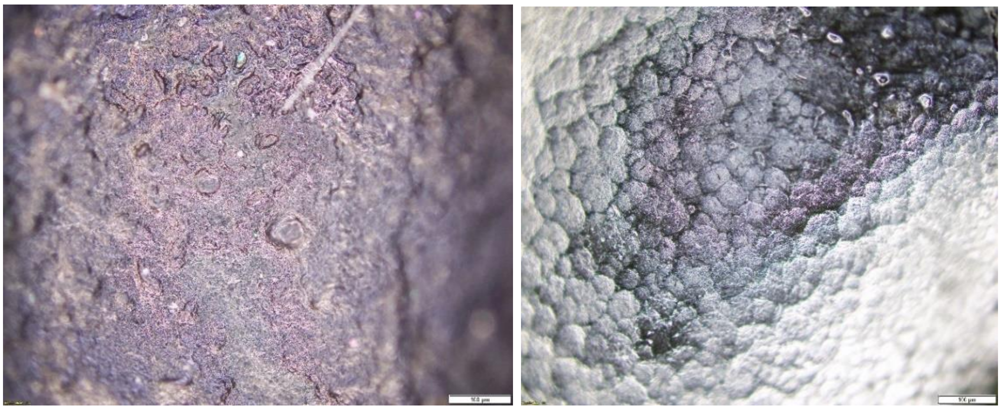

(a) (b)

Figure 4.73. N18 Microstructure After Pyrolysis a) Internal Structure b) External Structure

For the microstructure of the M7 material with test number N5, it was exposed to a temperature of 600 °C. Hollow charred structures were formed. Similar results were found by Zhang J. et al. (2018) [57]. It can be attributed to the fact that continued gas accumulation leads to increased pressure within the pores, causing these pores to continue to progressively develop and expand, ultimately leading to larger pore structures [59]. The pores formed on the surface of the N5 sample may indicate the release of H_2 gas. The study results have numerical results that can be examined numerically and experimentally in internal combustion engines.

N18 sample was blended with M7 material. Dense H_2 gas was observed in the sample. While the M7 material, which was exposed to heat along with the seed, did not release CH_4 gas by forming a layer on the surface, H_2 gas output was high.

Sample N16 is the sample that best exhibits CH_4 gas release. The seed exposed to heat without burning provided stable and regular gas release and showed regular pore formation.

Sample N6 was exposed to a temperature of 600 °C. It has been observed that low density and high viscosity polyethylene material provides H_2 gas release. In the experiment where high temperature was applied, the amount of seed carbonization increased and a result close to burning was observed in the microstructure.

The N8 sample is an experiment with a higher temperature difference than the N16 sample. The microstructure of the seed showed similar characteristics. Due to the oily structure in the seed at high temperatures, other gases other than CH_4 were also obtained. According to the results of the N16 sample of the experiment performed at 500 °C, a more stable and regular pore formation was observed in the microstructure of the N8 sample due to the increase in temperature [57].

The homogeneous distribution of gas outflows in the microstructure of the seed coat can be understood from the regular pore distribution on the surface. The surface of the sample is rough due to irregular organic structures. Many pores were also found, probably due to dissolution of functional structures [58].

5. CONCLUSION

In this study, obtaining biogas after pyrolysis of the Seed Bark of the Mediterranean Pine Tree (Turkish Pine), a member of the Pinus Pinea L. family growing in the Mediterranean Region of Turkey, and the usability of the obtained biogas as an energy source were investigated. In addition, in the study, biogas was obtained by mixing seed shells with polyethylene waste in different proportions. The effects of polyethylene materials on biomass were also observed.

- As a result of the analysis of the Mediterranean pine seed coat biomass N16 sample, it was determined that the CH_4 content was flammable gas.
- It has been determined that the gas obtained from Mediterranean pine seed bark biomass can be burned as an energy source.
- It has been observed that the temperature should not exceed 500 °C just to obtain CH_4 gas from the seed. The N16 test sample example proves this.
- It was determined that carbonization increased above 500 °C.
- It was determined that the amount of unidentified gas exceeded 500 °C.
- It was observed that H_2 dense gas was formed below 500 °C.
- When biomass is mixed with polyethylene materials, H_2 gas appears to play a dominant role.
- In the analysis of M7 polyethylene material, it was observed that the most intense H_2 gas release occurred.
- It has been determined that recycled polyethylene materials may still contain gas.
- It was observed that the gas release of pure polyethylene and seed mixture was rapid and could not be stored.
- As a result of N18 analysis, 70.77% H_2 gas was obtained. He showed that H_2 gas could be obtained at low temperature, even before pyrolysis was completed.
- According to the results, the highest CH_4 yield was reached in the N16 sample. In the gas property analysis, it was determined that 63.17% CH_4 was the most suitable gas in terms of flammability and usability instead of natural gas.
- N6 sample was analyzed as a mixture of 50% seed and M1 PE material. It consists of 21.78% CH_4, 55.03% CO_2 and 23.69% H_2. It was observed that with the addition of M1 material, the CH_4 ratio decreased and H_2 gas emerged.

- In the analysis of the N8 sample, the seed amount and temperature were increased by 100 °C compared to the N16 sample. Increasing the temperature to 600 °C caused the CH4 ratio to decrease and other gases to form.
- Sample N5 contains seedless catalyst. In order to better see the gas density, the M7 catalyst PE material, which has the highest density and lowest viscosity, was pyrolyzed. As a result of the experiment, 61.36% H_2 gas release was observed.
- It has been determined that the amount of H_2 gas obtained from Mediterranean pine seed shells can be used as an energy source.
- M7 HDPE material, with an MFI value of 0.45 g/10 min and a density value of 0.950 g/cm3, exhibited the best performance that can be used as a catalyst.

Gases from the findings of this study can be stored effectively and provide valuable information for future development efforts focused on improving the availability and performance efficiency of internal combustion engines. Subsequent research will investigate the potential of these gases in terms of performance and emissions of internal combustion engines.

REFERENCES

[1] Ravi R., Douadi O., Ezhilchandran M., Faqir M., Essadiqi E., Belkasmi M., Vijayalakshmi S.K., “A practical approach-based technical review on effective utilization of exhaust waste heat from combustion engines”, Energy Sources, Part A Recover. Util. Environ. Eff, 45, 10010–10033, 2023.

[2] Tang H., Dai Q., Cao Y., Li J., Wei X., Jibran K., Wang S., “Biomass and Bioenergy Production of jet fuel range hydrocarbons using a magnetic Ni – Fe / SAPO-11 catalyst for solvent-free hydrodeoxygenation of jatropha oil”, Biomass and Bioenergy, 177, 106927, 2023.

[3] Hepbasli A., Alsuhaibani Z., “Estimating and comparing the exergetic solar radiation values of various climate regions for solar energy utilization”, Energy Sources, Part A Recover. Util. Environ. Eff, 36, 764–773, 2014.

[4] Wang H., Wen C., Duan L., Li X., Liu D., Guo W., “Sustainable energy transition in cities: A deep statistical prediction model for renewable energy sources management for low-carbon urban development”, Sustainable Cities and Society Volume 107, 105434, 15 July 2024.

[5] Salem I., Saleh Y., Alsayed M. F., Assaf R., Kanan M., Al-Sartawi A. M., BinSaddig R., “Adoption of renewable energy sources and sustainable performance in palestinian industrial and commercial sectors with governmental role as a moderator: An explanatory approach”, Journal of Open Innovation: Technology, Market, and Complexity, 9, 100139, 2023.

[6] Soomro A., Chen S., Ma S., Sun Z., Xu C., Xiang W., “Promoting effect of ZrO2/CeO2 addition on Fe/CaO catalyst for hydrogen gas production in the gasification process”, Biomass and Bioenergy, 142, 2020.

[7] Data and statistics, Accessed: 3.5.2024. [Online]. Available: https://www.iea.org/data-and-statistics/charts?page=1.

[8] Cumulative renewable electricity capacity in the main and accelerated cases and Net

Zero Scenario. (2023). Accessed: 01.03.2024. [Online]. Available: https://www.iea.org/data-and-statistics/charts/cumulative-renewable-electricity-capacity-in-the-main-and-accelerated-cases-and-net-zero-scenario.

[9] Li P., Wang B., Hu J., Zhang Y., Chen W., Chang C., Pang S., “Research on the kinetics of catalyst coke formation during biomass catalytic pyrolysis: A mini review”, J. Energy Inst. 110, 101315.2023.

[10] Liu Y., Chen T., Gao B., Meng R., Zhou P., Chen G., Zhan Y., Lu W., Wang H., “Comparison between hydrogen-rich biogas production from conventional pyrolysis and microwave pyrolysis of sewage sludge: is microwave pyrolysis always better in the whole temperature range?”, Int. J. Hydrogen Energy. 46, 23322–23333. 2021.

[11] Balasundram V., Ibrahim N., Kasmani R. M., Hamid K. A., Isha R., Hasbullah H., Rasit Ali R., “Catalytic pyrolysis of sugarcane bagasse over cerium (rare earth) loaded HZSM-5 zeolite”, 9th International Conference on Applied Energy, ICAE2017, 21-24 August 2017, Cardiff, UK, Energy Procedia 142, 801-808. 2017.

[12] Chiodo V., Zafarana G., Maisano S., Freni S., Urbani F., ”Pyrolysis of different biomass: Direct comparison among Posidonia Oceanica, Lacustrine Alga and White-Pine”, Fuel. 164, 220–227. 2016.

[13] Al-fatesh A.S., Al-garadi N.Y.A., Osman A.I., Al-mubaddel F.S., Ibrahim A.A., Khan W.U., Alanazi Y.M., Alrashed M.M., Alothman O.Y., “From plastic waste pyrolysis to Fuel : Impact of process parameters and material selection on hydrogen production”, Fuel. 344, 128107. 2023,

[14] Shafizadeh A., Rastegari H., Shahbeik H., Mobli H., Pan J., Peng W., Li G., Tabatabaei M., Aghbashlo M., “A critical review of the use of nanomaterials in the biomass pyrolysis process”, J. Clean. Prod. 400, 136705. 2023.

[15] Oni B.A., Sanni S.E., Ibegbu A.J., Tomomewo O.S., Dike H.N., “Pyrolytic-gasification of biomass and plastic accompanied with catalytic sequential tar reformation into hydrogen-rich gas”, J. Energy Inst. 109, 101287.2023.

[16] Tian Y., He D., Zeng Y., Hu L., Du J., Luo Z., Ma W., Zhang Z., "Experimental research on hydrogen-rich syngas yield by catalytic biomass air-gasification over Ni/olivine as in-situ tar destruction catalyst", J. Energy Inst. 108, 101263. 2023.

[17] Acevedo-Paez J.C., Arenas-Castiblanco E., Posso F., Alarcón E., Villa A.L., Jahromi H., Adhikari S., "Effect of calcium and potassium on activity of mordenite-supported nickel catalyst for hydrogen production from biomass gasification", Int. J. Hydrogen Energy. 2023.

[18] Yue W., Ma X., Yu Z., Liu H., Li M., Lu X., "Ni-CaO bifunctional catalyst for biomass catalytic pyrolysis to produce hydrogen-rich gas", J. Anal. Appl. Pyrolysis. 169, 105872. 2023.

[19] Robinson O.J., Tewkesbury A., Kemp S., Williams I.D., "Towards a universal carbon footprint standard: a case study of carbon management at universities", J. Clean. Prod. 172, 4435-4455. 2018.

[20] Fu Y., Yu Y., Qiang J., Deng Y., Ren S., Elshareef H., Li H., Dong R., Zhou Y., "Experimental study on the regulation of NO_X in co-pyrolysis of maize straw and woody biomass", Fuel. 357, 129481. 2024.

[21] Li A., Han H., Zheng K., Zhu M., Xu K., Xu J., Jiang L., Wang Y., Su S., Hu S., Xiang J., "Sludge pyrolysis integrated biomass gasification to promote syngas: Comparison of different biomass", Fuel. 908, 168278. 2024.

[22] Wu Q., Huang W., Dai A., Ke L., Zhang L., Zhang Q., Cui X., Fan L., Xu C., Cobb K., Zou R., Pan X., Liu Y., Ruan R., Wang Y., "Two-step fast pyrolysis of torrefied corncobs and waste cooking oil under different atmosphere for hydrocarbons production", Energy. 286, 129535. 2024.

[23] Chen Y., Wang Z., Chen G., Wang Q., Sun T., Zhang M., Du Z., Wu M., Guo S., Lei T., Burra K.G., Gupta A.K., "Synergistic effects and products yield analyses based on co-pyrolysis of poplar tree and rape stalks with polyethylene terephthalate and polypropylene", J. Energy Inst. 112, 101461. 2024.

[24] Yu Y., Li X., Shao S., Zhang P., Jiang J., "Hydrogen production via biomass fast pyrolysis and in-line steam reforming using carbon reduced cathode material of spent $LiCoO_2$ batteries as catalyst", Fuel. 357, 129659. 2024.

[25] Parparit E., Brebu M., Uddin M. A., Yanik J., Vasile C., "Pyrolysis behaviors of various biomasses", Polymer Degradation and Stability 100 1-9.2024.

[26] Elleuch A., Halouani K., Li Y., "Exploration of Complex Electrochemical and Chemo-mechanical Behavior of SolidOxide Fuel Cell Fueled with Pyrolysis Bio-oil", Fuel Cells 18, No. 2, 206–218. 2018.

[27] Özbay G., "Catalytıc Pyrolysıs Of Pıne Wood Sawdust To Produce Bıo-Oıl: Effect Of Temperature And Catalyst Addıtıves", Journal of Wood Chemistry and Technology, 35:302–313.2015.

[28] Özçifçi A., Özbay G., "Mobilya Endüstrisi Atıklarından Katalitik Piroliz Yöntemi İle Biyoyakıt Üretimi", Journal of the Faculty of Engineering and Architecture of Gazi University, Vol 28, No 3, 473-479. 2013.

[29] Brebu M., Ucar S., Vasile C., Yanik J., "Co-pyrolysis of pine cone with synthetic polymers", Fuel 89 1911–1918. 2010.

[30] Bartolucci L., Cordiner S., Mele P., Mulone V., "Defatted Spent Coffee Grounds Fast Pyrolysis Polygeneration System: Lipid Extraction Effect On Energy Yield And Products Characteristics", Biomass and Bioenergy Volume 179, December 2023, 106974. 2023.

[31] Hu B., Liu J., Xie W., Li Y., Lu Q., "Chapter 6 - Biofuels production using pyrolysis techniques," Advances in Biofuels Production, Optimization and Applications, Pages 103-125. 2024.

[32] Zhanga, J., Tahmasebia, A., Omoriyekomwana, J. E., Yu, J., "Direct synthesis of hollow carbon nanofibers on bio-char during microwave pyrolysis of pine nut shell", Journal of Analytical and Applied Pyrolysis 130, 142–148. 2018.

[33] Tunç, N., Karagöz, M., Çiftçi, B., Deniz, E., “Environmental pollution cost analysis of a diesel engine fueled with biogas-diesel-tire pyrolytic oil blends”, Engineering Science and Technology an International Journal. 2020.

[34] Yılgın, M., Duranay, N. D., Pehlivan, D., “Odunun Flash Pirolizi”, Yeksem III. Yenilenebilir Enerji Kaynakları Sempozyumu, Mersin, Türkiye. 2005.

[35] Vita, A., Pino, L., Cipitì, F., Laganà, M., Recupero V., “Biogas as renewable rawmaterial for syngas production by tri-reforming process over NiCeO2 catalysts: Optimal operative condition and effect of nickel content”, Fuel Processing Technology, 127, 47–58. 2014.

[36] Yılmaz, İ. T., “Effect of Using Dual Fuel (Biogas-Diesel) on The Performance and Emissions of A Low Heat Rejection Diesel Engine”, Marmara University Institute For Graduate Studies In Pure And Applied Sciences. 2015.

[37] Sohaib, Q., Habib, M., Shah, S. F. A., Habib, U., Ullah, S., “Fast pyrolysis of locally available green waste at different residence time and temperatures”, Energy Sources, Part A: Recovery, Utılızatıon, And Envıronmental Effects. 2017.

[38] Olgun, A., “Pyrolysis of Some Biomass and The Investigation of Pyrolysis Products”, Ankara University Graduate School of Natural and Applied Sciences Department of Chemical Engineering. 2005.

[39] Olgun, H., Doğru, M., Howarth, C. R., “Katı Atıkların Enerji Dönüşümünde Kullanılması ve Gazlaştırıcılar”, IV. Ulusal Tesisat Mühendisliği Kongresi ve Sergisi. 2000.

[40] Morin, M., Pécate, S., Hemati, M., Kara, Y., “Pyrolysis of biomass in a batch fluidized bed reactor: Effect of the pyrolysis conditions and the nature of the biomass on the physicochemical properties and the reactivity of char. Journal of Analytical and Applied Pyrolysis”, Elsevier, 122, pp.511-523. 2018.

[41] Uludamar, E., Aydın, K., Özcanlı, M., “Noise and Exhaust Emission Characteristic of a Diesel Engine Fuelled with Natural Gas and Blends of Biodiesel and Diesel Fuels”, Karaelmas Fen ve Müh. Derg., 9(2):244-252. 2019.

[42] Gök, E., Taşar, Ş., Yılgın, M., Duranay, N. D., “Odun Peletlerinin Sabit Yatakta Yavaş Pirolizi”, Dokuzuncu Ulusal Kimya Mühendisliği Kongresi. 2010.

[43] Şensöz, S. & Can M., “Pyrolysis of Pine (Pinus Brutia Ten.) Chips:1. Effect of Pyrolysis Temperature and Heating Rate on the Product Yields Energy Sources”, 24:347–355. 2002.

[44] Erşen, T., Pehlivan, D., “Yüksek Yoğunluklu Polietilen–Odun Karışımlarının Birlikte Pirolizi”, Gazi Üniv. Müh. Mim. Fak. Der., Cilt 26, No 3, 607-612. 2011.

[45] Sağlamtimur, N. D., Bilgil, A., Çalışkan, Ö., Vural, T., Aykanat, T., Yolcu, F., “Ömrünü Tamamlamış Lastik Ve Polietilen Tereftalat (Pet) Şişe Atıklarının Pirolizinin Tasarlanan Yeni Bir Reaktörde Kıyaslanması”, Ömer Halisdemir University Journal of Engineering Sciences, Volume 6, Number 1, 21-27. 2017.

[46] Demiral, İ., Atilgan, N. G., Şensöz, S., “Productıon Of Bıofuel From Soft Shell Of Pıstachıo (Pıstacıa Vera L.)”, Chem. Eng. Comm., 196:104–115. 2008.

[47] Okay, G., Taşar, Ş., Yılgın, M., Duranay, N. D., “Çam Ve Kavak Ağacı Odunlarının Sabit Yatakta Ani Pirolizi”, Dokuzuncu Ulusal Kimya Mühendisliği Kongresi. 2009.

[48] Üçgül, İ., Elibüyük, U., “Tekstil Atıklarının Piroliz ile Değerlendirilmesi”, Journal of Technical Sciences, 4 (2) 40-46. 2014.

[49] Tabakaev, R. B., Astafev, A. V., Dubinin, Y. V., Yazykov, N. A., Zavorin, A.S., Yakovlev, V.A., “Autothermal pyrolysis of biomass due to intrinsic thermal decomposition effects”, Journal of Thermal Analysis and Calorimetry. 2018.

[50] Budak, M.S., “Biofuel Production By Rapid Pyrolysis Method Using Biomass”, Sakarya Üniversitesi Fen Bilimleri Enstitüsü, Yüksek Lisans Tezi. 2017.

[51] Ingemarsson, A., Nilsson, U., Nilsson, M., Pedersen, J. R., Oisson, J.O., "Slow Pyrolysis of Spruce and Pine Samples Studied with Gc/Ms and Gc/Ftir/Fid", Chemosphere, Vol. 36, No. 14, pp. 2879-2889. 1998.

[52] Zhoua N., Zhoub J., Daia L., Guoc F., Wangd Y., Lia H., Denga W., Leig H., Chena P., Liuc Y., Ruana R., "Syngas production from biomass pyrolysis in a continuous microwave assisted pyrolysis system", Bioresource Technology, 314, 123756. 2020.

[53] Anşin R., Özkan Z.C., "Tohumlu bitkiler (spermatophyta) odunsu taksonlar", second ed., KTU, Turkey, 1997.

[54] Zuleta A., Weisstaub A., Giacomino S., Dyner L., Loewe V., Del Rio R., Lutz M., "An ancient crop revisited: chemical composition of mediterranean pine nuts grown in six countries", Ital. J. Food Sci. 30, 170-183. 2018.

[55] Chu Z., Li Y., Zhang C., Fang Y., Zhao J., "A review on resource utilization of oil sludge based on pyrolysis and gasification", J. Environ. Chem. Eng., 11, 109692. 2023.

[56] Ball, M., Weeda, M. & Veziroğlu, N.T., "Compendium of Hydrogen Energy: Hydrogen Use, Safety and the Hydrogen Economy (Woodhead Publishing Series in Energy)", 1 St Edition Woodhead Press, Miami, FL, USA. 2016.

[57] Zhang J., Tahmasebi A., Esohe J., Yu J., "Direct synthesis of hollow carbon nano fibers on bio-char during microwave pyrolysis of pine nut shell", J. Anal. Appl. Pyrolysis, 130, 142–148. 2018.

[58] Li J., Burra K.R.G., Wang Z., Liu X., Gupta A.K., "Co-gasification of high-density polyethylene and pretreated pine wood", Appl. Energy, 285, 116472. 2021.

[59] Mu L., Wang R., Xie P., Li Y., Huang X., Yin H., Dong M., "Comparative investigation on the pyrolysis of crop, woody, and herbaceous biomass: Pyrolytic products, structural characteristics, and CO2 gasification", Fuel, 335,126940. 2023.

[60] Iwasaki, W., "A consideration of the economic efficiency of hydrogen production from biomass", Int. J. Hydrogen Energy, 28 (9); 939- 944. 2003.

VITA

Publication Produced from This Thesis:

Yönet N., Uludamar E., “Effect Of Recycled Polyethylene Catalyst For Mediterranean Pine Seed Shell Biomass Pyrolysis On Hydrogen And Methane Production”, Energy Sources, Part A: Recovery, Utilization, and Environmental Effects Volume 46, 6555-6565, 2024.

Publications:

Yönet N., Özdil N. F., “Investigation Of The Mixture Of Diesel And Fuel Marker Products In The Pipeline And In Tank Without Mixer”, Mas International European Conference On Mathematicsengineering- Natural & Medical Sciences-Xii, 246-254, 2020.

Yönet N., Özdil N. F., “Investigation Of Fluid Heat Transfer In Single Inlet Double Outlet T Pipe System”, Mas International European Conference On Mathematicsengineering- Natural & Medical Sciences-Xii, 238-245, 2020.

Arat H. T., Tanç B., Yönet N., Baltacioğlu E., “Comparative Simulation Analyses On Energy Flow Characteristics of Different Hev Configurations”, 16th International Conference on Clean Energy (ICCE-2018) 9-11 May 2018, Famagusta, N. Cyprus, 2018.

Yönet N., Tanç B., Arat H. T., “Effects Of Using Different Electric Motors On Hybrid Engine’s Performance”, 6 Th. International Conference On Renewable Fuels Combustion And Fire, 185-192, 2017.